

MICROCOPY RESOLUTION TEST CHART
NATIONAL BUREAU OF STANDARDS-1963-A

2

USAF-TR-85-3

AD-A159 319

UNITED STATES AIR FORCE ACADEMY

DEPARTMENT OF CHEMISTRY RESEARCH:

AY 1983 - 84

JULY 1985



APPROVED FOR PUBLIC RELEASE; DISTRIBUTION UNLIMITED

DTIC FILE COPY

DEAN OF THE FACULTY
UNITED STATES AIR FORCE ACADEMY
COLORADO SPRINGS, CO 80840

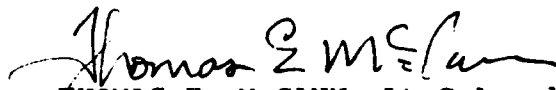
DTIC
ELECTE
SEP 19 1985
S D

85 09 04 062

This research report is presented as a competent treatment of the subject, worthy of publication. The United States Air Force Academy vouches for the quality of the research, without necessarily endorsing the opinions and conclusions of the author.

This report has been cleared for open publication and/or public release by the appropriate Office of Information in accordance with AFR 190-1 and AFR 12-30. There is no objection to unlimited distribution of this report to the public at large, or by DDC to the National Technical Information Service.

This research report has been reviewed and is approved for publication.



THOMAS E. McCANN, Lt Colonel, USAF
Director of Research and Computer-Based Education

UNCLASSIFIED

AD-A159 319

SECURITY CLASSIFICATION OF THIS PAGE

REPORT DOCUMENTATION PAGE

1a. REPORT SECURITY CLASSIFICATION UNCLASSIFIED		1b. RESTRICTIVE MARKINGS		
2a. SECURITY CLASSIFICATION AUTHORITY		3. DISTRIBUTION/AVAILABILITY OF REPORT This document has been approved for public release and sale; its distribution is unlimited.		
2b. DECLASSIFICATION/DOWNGRADING SCHEDULE				
4. PERFORMING ORGANIZATION REPORT NUMBER(S) USAFA-TR-85-3		5. MONITORING ORGANIZATION REPORT NUMBER(S)		
6a. NAME OF PERFORMING ORGANIZATION Department of Chemistry Dean of the Faculty	6b. OFFICE SYMBOL (If applicable) USAFA/DFC	7a. NAME OF MONITORING ORGANIZATION		
6c. ADDRESS (City, State and ZIP Code) U.S. Air Force Academy Colorado Springs, CO 80840		7b. ADDRESS (City, State and ZIP Code)		
8a. NAME OF FUNDING/SPONSORING ORGANIZATION Frank J. Seiler Research Lab	8b. OFFICE SYMBOL (If applicable)	9. PROCUREMENT INSTRUMENT IDENTIFICATION NUMBER		
8c. ADDRESS (City, State and ZIP Code) United States Air Force Academy Colorado Springs, CO 80840		10. SOURCE OF FUNDING NOS.		
		PROGRAM ELEMENT NO.	PROJECT NO.	TASK NO.
11. TITLE (Include Security Classification) United States Air Force Academy Department of Chemistry Research: AY 1983-84 (U)				
12. PERSONAL AUTHOR(S) Davis, Larry P., Major, Editor				
13a. TYPE OF REPORT Final	13b. TIME COVERED FROM 1Jun83 TO 31May84	14. DATE OF REPORT (Yr., Mo., Day) 85 July	15. PAGE COUNT	
16. SUPPLEMENTARY NOTATION				
17. COSATI CODES		18. SUBJECT TERMS (Continue on reverse if necessary and identify by block number) Chemical Research, Energetic Materials, Catalysis, Inorganic Chemistry, Biochemistry, Theoretical Chemistry		
FIELD	GROUP			SUB. GR.
7	02			Inorganic Chem
7	03	Organic Chem		
19. ABSTRACT (Continue on reverse if necessary and identify by block number) Department of Chemistry research during AY 1983-84 has progressed well in the areas of energetic materials, theoretical chemistry, and catalysis research. Working closely with Frank J. Seiler Research Laboratory on many of these projects, department researchers have synthesized new energetic compounds. Theoretical methods have been used to study basic silicon chemistry and biochemical molecules. Spectroscopic studies of the photodegradation of riboflavin have lead to an understanding of this important photochemical reaction. <i>Contents of this report include:</i>				
20. DISTRIBUTION/AVAILABILITY OF ABSTRACT UNCLASSIFIED/UNLIMITED <input checked="" type="checkbox"/> SAME AS RPT <input checked="" type="checkbox"/> DTIC USERS <input type="checkbox"/>		21. ABSTRACT SECURITY CLASSIFICATION UNCLASSIFIED		
NAME OF RESPONSIBLE INDIVIDUAL Major Larry P. Davis		22b. TELEPHONE NUMBER (Include Area Code) (303) 472-2681	22c. OFFICE SYMBOL HQ USAFA/DFC	

UNITED STATES AIR FORCE ACADEMY

Department of Chemistry Research:

AY 1983-84

Major Walter B. Avila
Lieutenant William Beninati
Major Larry W. Burggraf
Major Larry P. Davis
Lieutenant Thomas A. Erchinger
Major Dennis J. Fife
Lieutenant Gary M. Gfeller
Lieutenant Kevin A. Lang
Dr. Charles N. Robinson
Captain Larry D. Strawser

Compiled and Edited
by
Major Larry P. Davis

July
~~April~~ 1985

Accession #	
NTIS GRA&I	<input checked="" type="checkbox"/>
DTIC TAB	<input type="checkbox"/>
Unannounced	<input type="checkbox"/>
Justification	
<i>Rec'd date needed per telegram.</i>	
<i>J.C.</i>	
Distribution/	
Availability Codes	
Dist	Avail and/or Special
<i>A-1</i>	



Preface

This technical report outlines the Department of Chemistry research efforts for academic year 1983-84. Each chapter covers specific accomplishments of one particular research product. It is the second of an annual department technical report. It was compiled and edited by Major Larry P. Davis, the DFC Director of Research. Authors would like to thank Mrs. Pat Ridley for the expert typing.

Abstract

Department of Chemistry research during AY 1983-84 has progressed well in the areas of energetic materials, theoretical chemistry and catalysis research. Working closely with Frank J. Seiler Research Laboratory on many of these projects, department researchers have synthesized new energetic compounds. Theoretical methods have been used to study basic silicon chemistry and biochemical molecules. Spectroscopic studies of the photodegradation of riboflavin have led to an understanding of this important photochemical reaction.

TABLE OF CONTENTS

	Page Number
Chapter 1. ^{const} Synthesis of Polynitrophenyl Acetylenes..... Walter B. Avila and Thomas A. Erchinger	1
Chapter 2. Regiospecific Fluorination of Aryl Anions with Xenon Difluoride..... Walter B. Avila and Kevin A. Lang	24
Chapter 3. ^{const} Correlation of ¹³ C Constants with NMR Chemical Shifts in Fluorine, Phosphorus, and Nitrogen-Containing Styrene Derivatives..... Charles N. Robinson	31
Chapter 4. Photodegradation of Riboflavin..... Dennis J. Fife and Gary M. Gfeller	53
Chapter 5. A Quantum-Chemical Study Relating Pseudorotation to the Stereochemistry of Nucleophilic Substitution at Silicon..... Larry W. Burggraf and Larry P. Davis	63
Chapter 6. Theoretical Calculations of the Peptide Bond..... Larry D. Strawser, Larry P. Davis, and William Beninati	92

CHAPTER 1

SYNTHESIS OF POLYNITROPHENYL ACETYLENES

Walter B. Avila and Thomas A. Erchinger

ABSTRACT

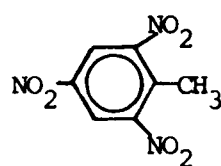
Development of methods to synthesize polynitrophenyl acetylenes are in progress. This paper presents the initial literature research and the preliminary laboratory results. The two target molecules selected for the initial investigation are 2,4,6-trinitrophenylacetylene and 2,2',4,4',6,6'-hexanitrodiphenylacetylene.

INTRODUCTION

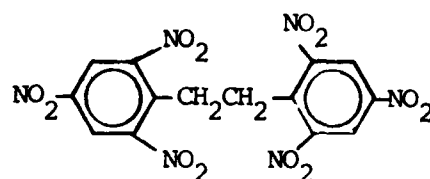
Polynitrophenyl compounds are of interest as energetic materials for high-energy applications such as propellants and explosives. Continued research has been directed toward the synthesis of energetic materials having enhanced physical properties. These physical properties include increased thermal stability and higher energy output.

Currently 2,4,6-trinitrotoluene (TNT) is the most widely used energetic material. 2,2',4,4',6,6'-Hexanitrophenylethane (hexanitrobibenzyl, HNBB) and 2,2',4,4',6,6'-hexanitrodiphenylethane (hexanitrostilbene, HNS) are readily produced from TNT. Synthesis of 2,2',4,4',6,6'-hexanitrodiphenylethyne (hexanitrotolane, HNT) would complete the homologous series of HNBB, HNS, and HNT. Both HNBB and

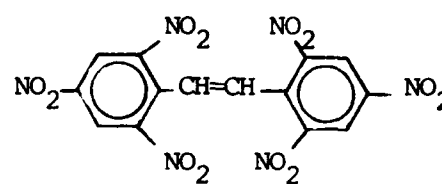
HNS exhibit high energy characteristics, and HNS showed an increased thermal stability over HNBB. It is expected that HNT might show even better thermal stability with still higher energy output. 2,4,6-Trinitrophenylacetylene (TNPA) is of interest as an explosive and possibly an intermediate in the synthesis of HNT.



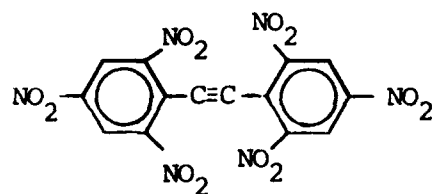
TNT



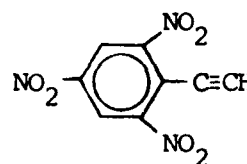
HNBB



HNS



HNT

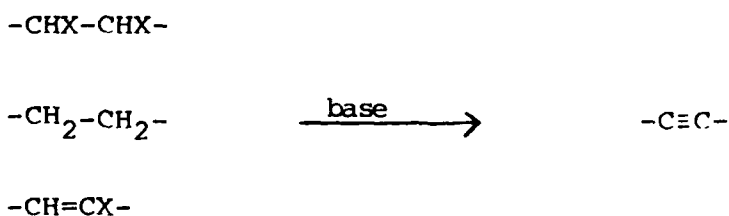


TNPA

Since the carbon-carbon triple bond is the major functionality in the desired target molecules an extensive background search was initiated on the newer methods for the preparation of alkynes developed since 1970. There have been numerous methods for the preparation of substituted alkynes starting with alkynes,¹⁹⁻²⁶ however, only material involving the carbon-carbon triple bond formation from acetylene itself or non-acetylene precursors is discussed.

BACKGROUND

The first preparation¹ of an alkyne was that of acetylene in 1837 by E. Davy. This was followed shortly thereafter by the preparation of the substituted acetylene propyne in 1861. Alkynes have traditionally been synthesized by elimination reactions² represented as

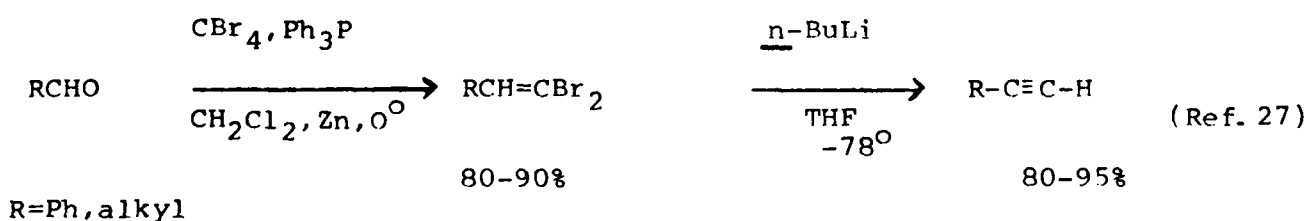


where X is a halogen or an equivalent leaving group and the reagent is a strong base. Additionally, alkylation of metal acetylides has been used as a primary synthetic route for the preparation of substituted acetylenes. These types of reactions, as well as the early synthetic methodology, are presented in several texts and reviews.²⁻⁷

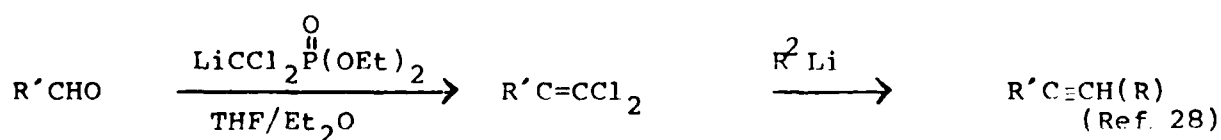
In 1950 there were only about seven naturally occurring acetylenes.² This had increased to more than 450 in 1969² and to well over 1000 by 1970. Interest in carbon-carbon triple bond formation increased with the discovery of new natural products. Synthetic methodology was needed not only to prepare the acetylenic natural products themselves, but also to prepare the alkynes used as the key intermediates in the synthesis of pheromones¹², steroids^{13,14}, ter-

penoids¹⁵, sesquiterpenes¹⁶, prostaglandins¹⁷, and numerous other naturally occurring materials.¹⁸ The more recent isolation and identification of naturally occurring acetylenes and acetylene containing natural products are given in references 8-11.

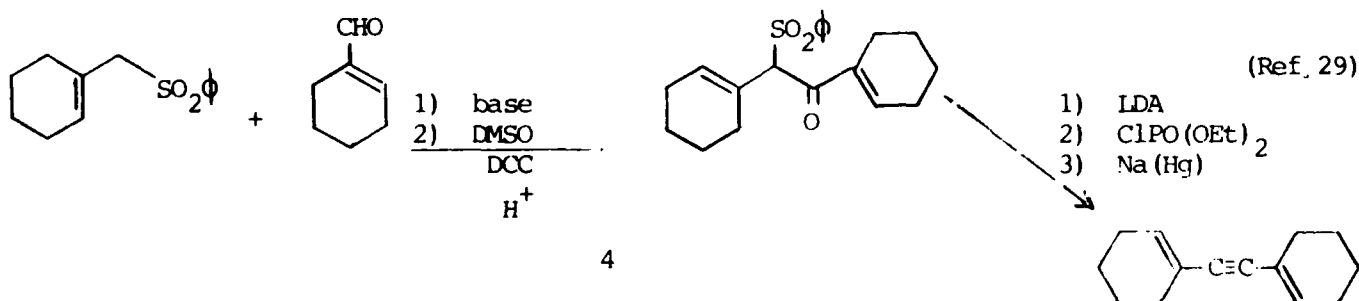
The formation of carbon-carbon triple bonds from aldehydes⁴⁵ is best exemplified by the efforts of Corey²⁷ as shown below.



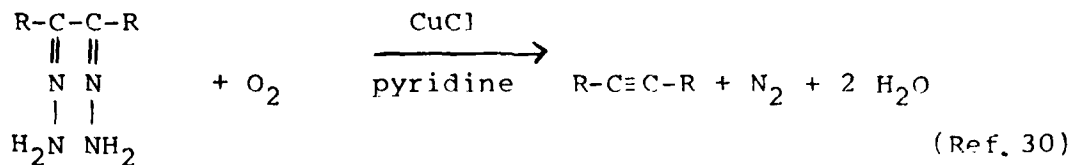
Alkynes prepared by this procedure were subsequently used in a variety of synthetic procedures including the synthesis of prostaglandins. A modification of the above transformation was subsequently developed²⁸ and involves the synthesis of conjugated



enynes from α,β -unsaturated aldehydes.²⁹

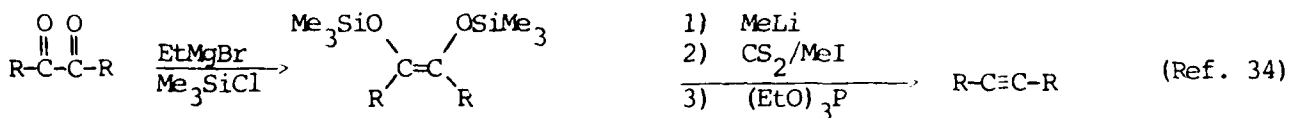


The conversion of ketones to carbon-carbon triple bonds have been looked at by several groups. Tsuji and co-workers^{30,44} have converted 1,2-diketones to acetylenes via their hydrazones.

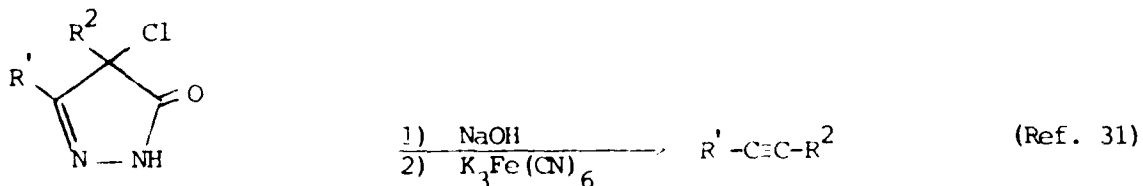


R=alkyl, aryl

In their quest for routes to novel cyclic acetylenes, Bauer and Macomber³⁴ used 1,2-diketones (and esters) to form carbon-carbon triple bonds.



Likewise, 1,3-diketones³¹ were converted to alkynes via their 4-chloro-2-pyrazolin-5-one derivatives.



R' or R² = alkyl, aryl

REFERENCES

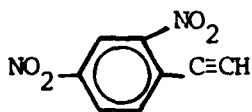
1. E. Davy, Annalen, 23, 144 (1837).
2. J. C. Craig, M. D. Bergental, I. Fleming, and J. Harley-Mason, Angew. Chem. Int. Ed., 8, 429 (1969).
3. H. G. Viehe, Chemistry of Acetylenes, Marcel-Dekker, Inc., New York, 1969.
4. T. F. Rutledge, Acetylenes and Allenes, Reinhold Book Corp., New York, 1969.
5. T. F. Rutledge, Acetylenic Compounds, Reinhold Book Corp., New York, 1968.
6. T. L. Jacobs, Organic Reactions, 5, Chapter 2, Wiley and Sons, Inc., New York, 1949.
7. G. Kobrich, Angew. Chem. Int. Ed., 4, 49 (1965).
8. T. B. Patrick and G. F. Melm, J. Org. Chem., 44, 645 (1979).
9. A. F. Orr, JCS Chem. Comm., 40 (1979).
10. M. Ahmed, J. W. Keeping, T. A. Macrides, and V. Thaller, JCS Perkin I, 1487 (1978); L. W. Farrell, M. T. W. Hearn, and V. Thaller, ibid., 1485 (1978); D. G. Davies, P. Hodge, P. Yates, and M. J. Wright, ibid., 1602 (1978).
11. F. Bohlmann and C. Zdero, Phytochemistry, 17, 1595 (1978); F. Bohlmann and Wolf-Rainer Abraham, ibid., 1629 (1978); F. Bohlmann and U. Fritz, ibid., 1769 (1978).
12. C. A. Henrich, Tetrahedron, 33, 1845 (1977).
13. T. M. Dawson, J. Dixon, P. S. Littlewood, B. Lythgoe, and A. K. Saksena, JCS (C), 2960 (1971).
14. W. S. Johnson, L. R. Hughes, J. A. Kloek, T. Niem, and A. Shenvi, J. Am. Chem. Soc., 101, 1279 (1979); W. S. Johnson, L. R. Hughes, J. L. Carlson, ibid., 1281 (1979); W. S. Johnson, R. S. Brinkmeyer, V. M. Kapoor, and T. M. Yarnell, ibid., 99, 8341 (1977).
15. N. Okukado and Ei-ichi Negishi, Tetrahedron Lett., 2357 (1978).

-110°. n-Butyllithium (Aldrich, 1.58M in hexane, 1.00ml) was added to the acetylene flask and resulting monolithium acetylide transferred via cannula to the DNPA flask. After 10 minutes the reaction was quenched with methanol. Subsequent work-up gave .322g (quantative) of 2,4-dinitroanisole which was identified by comparison to an authentic sample.

The extracts were dried, filtered, and evaporated to give a black oil (0.760g). Separation using ethyl acetate/hexane (50/50) gave five fractions. NMR spectra on the evaporated fractions showed no desired product and no identifiable compounds.

In the second run, the reaction mixture at -110° was allowed to react for 2 minutes. The reaction was then quenched with 1ml of methanol. A dark red-brown solution still resulted. Ether (5ml) and 5ml of water were added, and the solution was allowed to warm to room temperature. The solution was worked up as above. The product was run through a short silica gel scrubber column using ethyl acetate. The eluents were evaporated and separated by MPLC using methylene chloride/hexane (20/80) for fractions 1 through 6; methylene chloride (100%) for fractions 7 through 12; and methylene chloride/ethyl acetate (90/10) for fractions 13 through 15. Data collected by GC/MS showed no desired product. PiCl starting material was present in fraction 3 (8mg, 1% of starting amount) ($m/e = 247$ and 109).

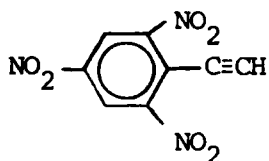
Attempted Synthesis of 2,4-Dinitrophenylacetylene



2,4-Dinitrofluorobenzene (Aldrich, .294g, 1.58mmol) was placed in a 50ml flask with a stir pea. The system was purged with argon then THF (5.0ml) and ether (2.0ml) were added. The reaction flask was cooled to -110° . Acetylene was slowly bubbled into ether (15ml) in a 25ml flask at

was dried and concentrated to give a yellowish-white solid (I, 0.723g, 87% yield). Mass spectral data confirmed the product was picryl chloride (molecular ion peaks at $m/e = 247$, and $m/e = 109$ for loss of three NO_2 groups).

Attempted Synthesis of 2,4,6-Trinitrophenylacetylene



An acetylene bulb was evacuated, tared, then filled with acetylene (Union Carbide, 0.0831g, 3.19mmol). THF (10ml) in a 25ml flask with a stir pea

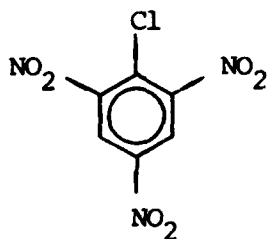
was cooled to -78° . Picl (0.7097g, 2.87mmol) was dissolved in 5ml THF in a 35ml flask with a stir pea and cooled to -110° . Acetylene was slowly bubbled into the THF at -78° for 15 minutes using argon pressure. *n*-Butyllithium (Aldrich, 1.63M in hexane-1.75ml, 2.84mmol) was added dropwise via syringe. No change in the reaction mixture was noticed. The solution at -78° was transferred dropwise via canula and positive argon pressure to the solution at -110° over a three-minute period. The solution immediately turned blood-red. The emptied flask was washed with 1ml THF, which was allowed to cool then was transferred to the second flask also. In the first run, the reaction mixture was allowed to warm to room temperature and react overnight. Water (10ml) and 30ml ether were added to the solution in a separatory funnel. Solid sodium chloride was added to facilitate separation. The solution was extracted twice with ether.

internal standard. Mass spectral data was obtained from a Hewlett-Packard 5985B GC/MS System with an HP 3-foot packed column of 2%-OV101 on 100-200 mesh Ultrabond 20M.

Solvents and Reagents

Tetrahydrofuran (THF) and ether were purified and distilled from the sodium-benzophenone ketyl immediately before use. Ethyl acetate, hexane, and methylene chloride used in MPLC were HPLC grade. *n*-Butyllithium was standardized using diphenyl acetic acid or 2,4-dimethoxybenzyl alcohol.⁶⁸

Picryl Chloride



Picric acid slurry (Aldrich, 65% picric acid, 35% water--1.74g, 4.49mmol) was dissolved in 12ml hot 95% ethanol in a 35ml flask with a stir pea. Pyridine (Eastman, 0.351g, 4.44mmol) was added via syringe with stirring. A yellow precipitate formed before all the pyridine was added. The solution was allowed to react for 10 minutes then it was vacuum filtered to give fine yellow needles of pyridine picrate (wet yield, 1.03g). Benzene (1ml) and POCl₃ (Baker, 0.31ml, 3.34mmol) were added to the pyridine picrate in a 10ml flask with a stir pea. The mixture was refluxed at 70° for 0.5h using an oil bath. The mixture liquefied upon heating, giving a clear, yellow solution. The solution was washed with two 5ml portions of hot water and the benzene/oil layer

EXPERIMENTAL

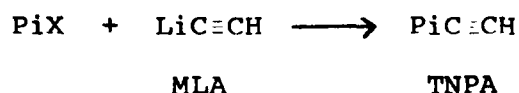
General

All temperatures are in degrees Celsius ($^{\circ}\text{C}$). All glassware was baked at 120° and allowed to cool in a dessicator. All oxygen and moisture-sensitive reactions were carried out under argon atmosphere with a positive argon pressure. Except where noted, all liquid reagents and solvents were added to reaction vessels via syringe through septums. All solvent evaporations were performed using a Buchi rotavapor. All analytical mass measurements were made on an Ainsworth Right-a-Weigh Analytical balance. Reactions at -78° were carried out in an acetone-dry ice bath. Reactions at -110° were run in an ether-liquid nitrogen bath. Acetylene (purified) was dispensed from a bottle (CO_2 /Acetone trap) into a two-ended bulb with stop cocks at each end. The acetylene was collected at atmospheric pressure. All extracts were dried with magnesium sulfate. Thin layer chromatography (TLC) was run on Eastman Kodak 6060 silica gel plates with fluorescent indicator. MPLC separations were carried out on a 22mm column with a short scrubber column using Woelm Pharma silica gel (particle size 32-63 μm). Pressure in the column was 20-30 psi. Fractions were distinguished using an Instrumentation Specialties Company (ISCO) Type 6 Optical Unit by measuring absorbances at 254nm. Absorbance data was collected on an ISCO Model UA-5 Absorbance Monitor. NMR spectra were collected on a JEOL FX90Q Fourier Transform NMR Spectrometer using tetramethylsilane as an

CONCLUSIONS

The literature survey of current synthetic methods provides for a sound and practical foundation for the preparation of energetic tolans. Initial experimentation while not furnishing any energetic materials has provided the necessary data for future success using the methods outlined above.

The obvious method for preparation of TNPA involves the nucleophilic substitution reaction of monolithium acetylide with a picryl halide as shown below

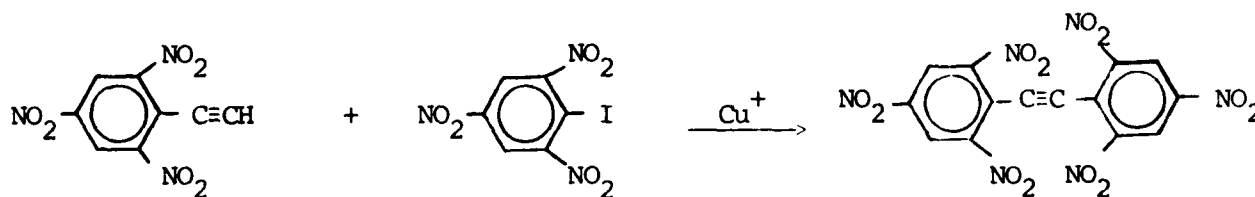


The MLA has been prepared by a variety of methods⁶⁴ and is well characterized.⁶⁴ It has further been shown that the nitro groups can stand the strong basic conditions if the temperature is kept below -100°C .⁶⁵ Picryl chloride was prepared in an 87% yield by the method of Boyer, Spenser and Wright.⁶⁶ This was reacted with MLA in THF at -110°C under a variety of reaction conditions. To insure that the MLA was indeed generated this reaction should be rerun using reference 64b to generate the MLA or using trimethylsilylacetylene to generate an acetylide ion equivalent.

Since the order of halide reactivity for $\text{S}_{\text{N}}\text{Ar}$ type reactions is $\text{F} \gg \text{Cl} > \text{Br} > \text{I}$ the reactivity of 2,4-dinitrofluorobenzene (DNFB) was investigated. Reaction of DNFB with MLA with subsequent quenching using methanol at -78°C gave 2,4-dinitroanisole as the major product. This indicates that either the MLA is not being formed or the MLA is very sluggish to react. Generation of MLA by the procedure outlined in reference 64b should eliminate the first problem. The reactivity of MLA could be enhanced by using HMPA⁶⁷ as a co-solvent or complexing with 18-crown-6.

The presence of more nitro groups in the hexanitro compounds is believed to prevent a similar reaction to produce HNT; however, different reaction conditions may allow formation of the dichloro compound from which HNT could be produced. The harsh conditions required for nitration prevent the formation of diphenylethyne (tolane). Under these conditions the carbon-carbon triple bond would be destroyed.

The second approach, combining functionally complete subunits to form HNT, is the primary route that is felt will offer the highest chance of success. This method would involve the reaction of trinitrophenylacetylene (TNPA) with a picryl halide to give HNT. To run the reaction, TNPA must first be converted to a cuprous acetylide, following the route of Stephens and Castro for the synthesis of diaryl acetylenes:⁶³



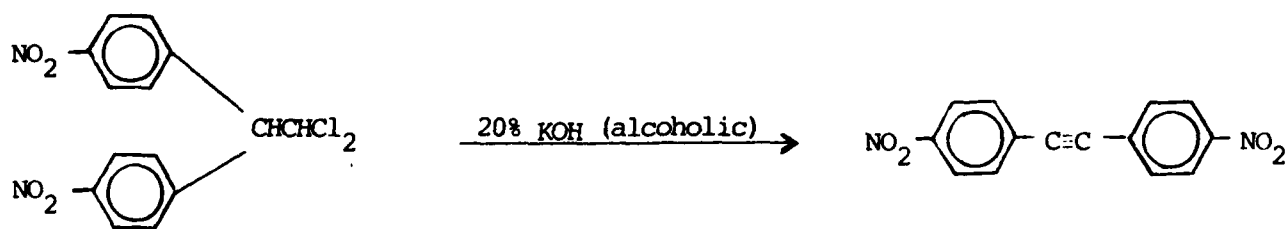
(Ref. 63)

Although picryl iodide (PiI) is a known substance, TNPA has not yet been produced. Therefore, synthetic efforts were directed toward the preparation of TNPA.

RESULTS AND DISCUSSION

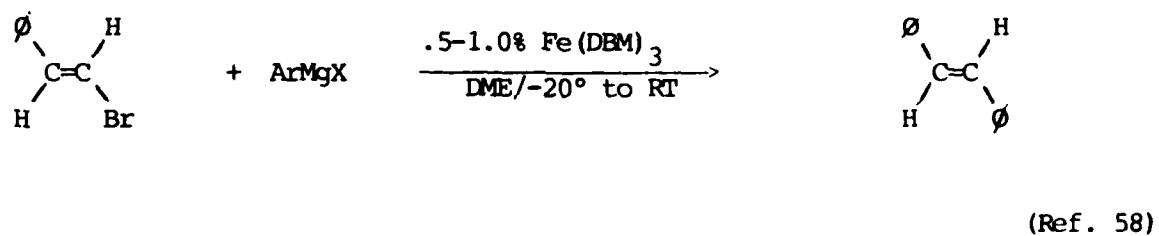
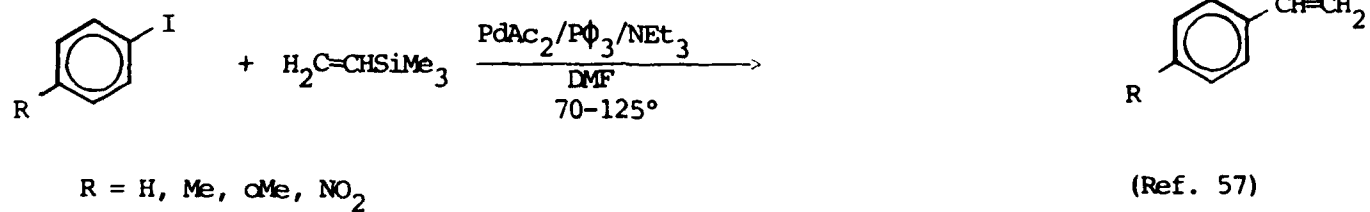
The ultimate goal of this project is to design an effective synthesis of HNT. Two general approaches to the problem can be taken. First, the 14-carbon structure of the molecule could be established then modified to produce the proper nitro and alkyne functional groups of HNT. Second, separate compounds already containing the proper functionality could be joined together to complete the HNT molecule.

Several attempts to synthesize HNT using the first approach have been unsuccessful. Halogenation of HNS using both bromine and chlorine (to be followed by dehydrohalogenation to form HNT) failed under numerous reaction conditions.^{60,61} HNBB also proved to be relatively unreactive towards chlorination of its aliphatic group. It should be pointed out, however, that R. Delaby and R. Baronnet reported a successful synthesis of 2,2'-dinitrotolane using a dehydrochlorination rearrangement reaction:⁶²



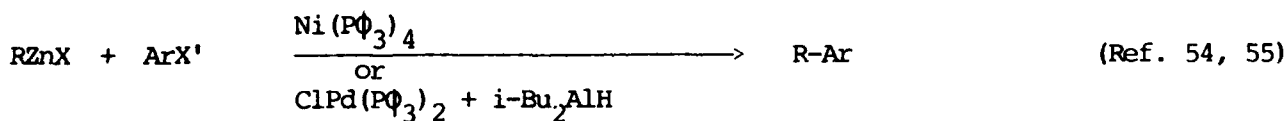
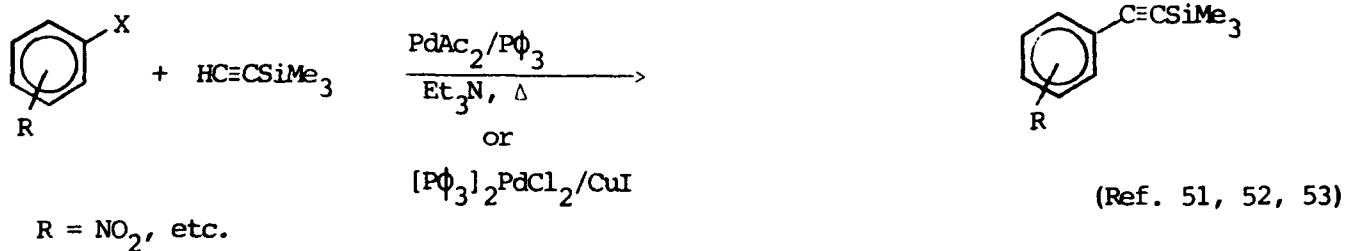
(Ref. 62)

Finally two methods of preparing alkenes^{57,58} offer potential for modification to prepare alkynes.



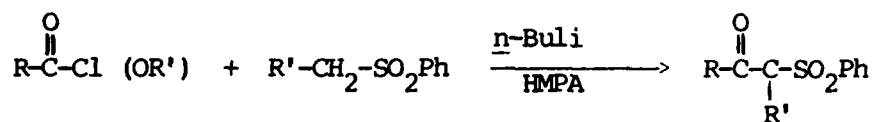
DBM = tris (dibenzoylmethido)

The above methods offer potential for the tolane syntheses, however, the recent literature has provided methodology which would on a whole offer more chances of success. Among these methods are some modifications to the classical dehalogenation⁴⁷ and dehydrohalogenation reactions.^{48,49} Also included are methods for preparing alkynes from α -acyl/ α -thio phosphoranes⁵⁰, from arylhalides, transition metal catalysts⁵¹⁻⁵⁶, and cuprates.⁵⁹



R = H, alkyl, aryl
 X = Br, Cl
 X' = Br, I





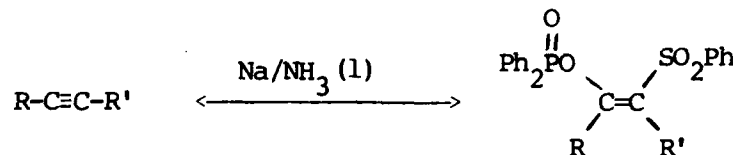
R = aryl, alkyl

R' = alkyl, H

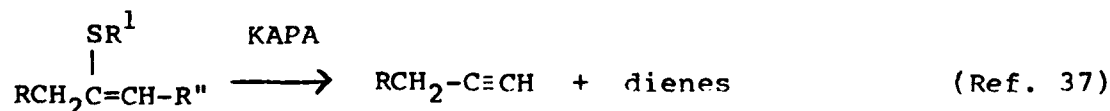


Ph₂POCl

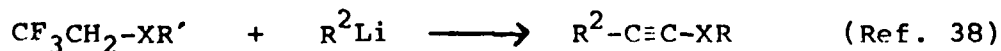
(Ref. 36)



Brown³⁷ has prepared terminal alkynes from vinyl sulfides by using his super base potassium 3-aminopropylamine (KAPA).



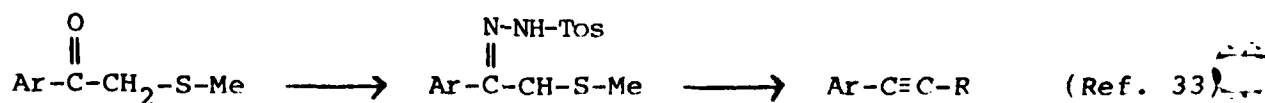
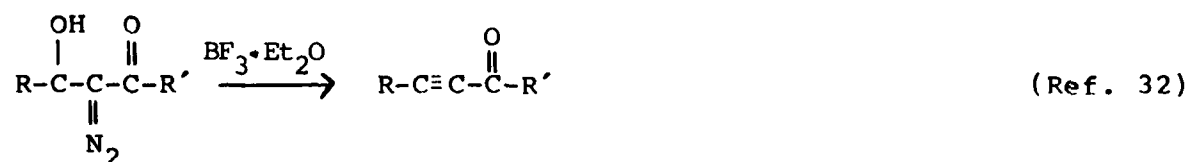
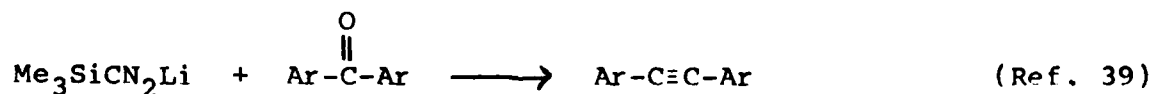
In their effort to demonstrate the utility of fluorine containing organic compounds, Tanaka and co-workers³⁸ have prepared alkynes from 2,2,2-trifluoroethyl ether and thioethers.



X = O, S

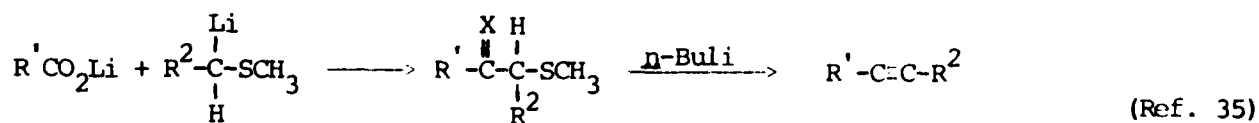
Finally, alkynes have been prepared from organic halides⁴⁰ by base elimination, from α,β -epoxy ketones^{41,42}, from α -bromoketones⁴³, and from 1,1-difluoroethene⁴⁶.

This procedure has found application in the synthesis of Junipal.³¹
 The conversion of ketones³⁹ to alkynes has been accomplished via
 diazoketones³² and β -ketosulfides.³³



R=H, Me

Carboxylic acids have been converted to alkynes by reaction
 with methylthiomethyl lithium.³⁵



R' = aryl, alkyl

X = O, N-NHTos

R² = Ph, H

In a somewhat similar manner, acid chlorides and esters³⁶ have been
 converted to alkynes by reaction with sulfones.

16. B. M. Trost, C. D. Shuey, F. Dininno, Jr., and S. S. McEluain, J. Am. Chem. Soc., 101, 1284 (1979).
17. R. S. Brinkmeyer and V. M. Kapoor, J. Am. Chem. Soc., 99, 8339 (1977).
18. Ka-Kong Chang, N. Cohen, J. P. Denobel, A. C. Specian, Jr., and G. Saucy, J. Org. Chem., 41, 3497 (1976); G. Buchi, H. Wuest, ibid., 44, 546 (1979); F. Bohlmann, F. Stohr, and J. Staffeidt, Chem. Ber., 111, 3146 (1978); A. Akhtar, A. E. Faruk, C. J. Harris, G. P. Moss, S. W. Russell, and B. C. L. Weedon, JCS Perkin I, 1511 (1978); A. Stutz and H. Reinshagen, Tetrahedron Lett., 2821 (1978).
19. L. Carlton and G. Read, JCS Perkin I, 1631 (1978); C. C. Bond and M. Hooper, JCS (C), 245 (1969); I. Fleming, C. R. Owen, ibid., 2013 (1971).
20. A. J. Quillinan, E. A. Khan, and F. Scheinmann, JCS Chem. Comm., 1030 (1974); R. S. Brinkmeyer and T. L. MacDonald, ibid., 876 (1978).
21. M. Naruse, K. Utimoto, H. Nozaki, Tetrahedron Lett., 1847 (1973); J. F. Normant, A. Commercon, and J. Villieras, ibid., 1468 (1975); J. C. Chabala and J. E. Vincent, ibid., 937 (1978); G. Giacomelli and L. Lardicci, ibid., 2831 (1978); C. C. Shen and C. Ainsworth, ibid., 83 (1979); G. Cassani, P. Hassardo, and P. Piccardi, ibid., 633 (1979).
22. M. Naruse, K. Utimoto, and H. Nozaki, Tetrahedron, 30, 2159 (1974); J. Klein and J. Y. Becker, ibid., 28, 5385 (1972).
23. W. Beckmann, G. Doerjer, E. Loemann, C. Merkel, G. Schiller, and C. Zurcher, Synthesis, 423 (1975); L. Lompa-Krzymein and L. C. Leitch, ibid., 124 (1976); K. Yamada, N. Miyaura, M. Itoh, and A. Sukuki, ibid., 679 (1977).
24. H. C. Brown, J. A. Sinclair, M. M. Midland, J. Am. Chem. Soc., 95, 3080 (1973); Ei-ichi Negishi and S. Baba, ibid., 97, 7385 (1975).
25. M. M. Midland, J. Org. Chem., 40, 2250 (1975).
26. J. N. Gardner, Can. J. Chem., 53, 2157 (1975).
27. E. J. Corey and P. L. Fuchs, Tetrahedron Lett., 3769 (1972).
28. J. Villieras, R. Perriot, and J. F. Normant, Synthesis, 458 (1975).

29. B. Lythgoe and I. Waterhouse, Tetrahedron Lett., 2625 (1978).
30. J. Tsuji, H. Takahashi, and T. Kajimoto, Tetrahedron Lett., 4573 (1973).
31. P. J. Kocienski, J. M. Ansell, and B. E. Norcross, J. Org. Chem., 41, 3650 (1976).
32. R. Pellicciari, E. Castagnino, R. Fringuelli, and S. Corsano, Tetrahedron Lett., 481 (1979); E. Wenkert and C. A. McPherson, Syn. Comm., 2, 331 (1972).
33. S. Kano, T. Yokomatsu, T. Ono, S. Hibino and S. Shibuya, Synthesis, 305 (1978).
34. D. P. Bauer and R. S. Macomber, J. Org. Chem., 41, 2640 (1976).
35. S. Kano, T. Yokomatsu, and S. Shibuya, J. Org. Chem., 43, 4366 (1978).
36. P. Bartlett, F. R. Green III, and E. H. Rose, J. Am. Chem. Soc., 100, 4852 (1978).
37. C. A. Brown, J. Org. Chem., 43, 3083 (1978).
38. K. Tanaka, S. Shiraishi, T. Nakai and N. Ishikawa, Tetrahedron Lett., 3103 (1978).
39. E. W. Colvin and B. J. Hamill, JCS Perkin I, 869 (1977).
40. J. R. Sowa, E. J. Lamby, E. C. Calamai, D. A. Benko, and A. Gordinier, Org. Prep. and Proc. Int., 7, 137 (1975).
41. P. Wieland, Helv. Chim. Acta., 53, 171 (1970).
42. E. J. Corey and H. S. Sachdev, J. Org. Chem., 40, 579 (1975).
43. M. W. Bryant, R. A. J. Smith, and L. Wong, Aust. J. Chem., 35, 2529 (1982).
44. J. Tsuji, H. Kezuka, Y. Toshida, H. Takayanagi, and K. Yamamoto, Tetrahedron, 39, 3279 (1983).
45. H. J. Bestmann and K. Li, Chem. Ber., 115, 828 (1982).
46. R. Sauvetre and J. F. Normant, Tetrahedron Lett., 23, 4325 (1982).

47. F. Sato, T. Akiyama, K. Iida, and M. Sato, Synthesis, 1025 (1982).
48. Y. Kimura and S. L. Regen, J. Org. Chem., 47, 2493 (1982); I. Yamawaki, T. Kawate, T. Ando, and T. Hanafusa, Bull. Chem. Soc. Jpn., 56, 1885 (1983).
49. A. Alberti and G. F. Pedulli, Tetrahedron, 38, 3605 (1982).
50. A. L. Braga, J. V. Comasseto, and N. Petragnani, Tetrahedron Lett., 25, 1111 (1984).
51. W. B. Austin, N. Bilow, W. J. Kelleghan, and K. S. J. Lav, J. Org. Chem., 46, 2280 (1981).
52. S. Takahashi, Y. Kuroyama, K. Sonogashira, and N. Hagihara, Synthesis, 627 (1980); J. Lindley, Tetrahedron Lett., 40, 1446 (1984).
53. K. Sonogashira, Y. Tohda and N. Hagihara, Tetrahedron Lett., 4467 (1975).
54. E. Negishi, A. O. King, and N. Okukado, J. Org. Chem., 42, 1821 (1977).
55. A. O. King and E. Negishi, J. Org. Chem., 43, 358 (1978).
56. A. N. Kashin, I. G. Bumagina, N. A. Bumagin, and I. P. Beletskaya, J. Org. Chem. (USSR), 17, 18 (1981).
57. A. Hallberg and C. Westerlung, Chem. Lett., 1993 (1982).
58. G. A. Molander, B. J. Rahn, D. C. Shubert, and S. E. Bonde, Tetrahedron Lett., 24, 5449 (1983).
59. C. C. Bond and M. Hooper, J. Chem. Soc. (C), 2453 (1969).
60. Keith C. Hansen, "Nitro Organic Compounds: A Synthetic Study", FJSRL Technical Memorandum 82-0020, August 1982.
61. Personal Communication with Dr. J. Wilkes, FJSRL, USAF Academy, CO 80840.
62. R. Delaby and R. Baronnet, Bull. Soc. Chim. Fr., 148 (1951); in Synthetic Methods, 7, p. 998.
63. R. D. Stephens and C. E. Castro, J. Org. Chem., 28, 3313 (1963).

64. a) M. M. Midland, J. Org. Chem., 40, 2250 (1975); b) See reference 55 - best method; c) W. Beckmann, G. Doerjer, E. Logemann, C. Merkel, G. Schill, C. Zurcher, Synthesis, 423 (1975).
65. a) W. E. Parham and R. M. Puccirilli, J. Org. Chem., 42, 257 (1977); b) G. Kobrich and P. Buck, Chem. Ber., 103, 1412 (1970).
66. R. Boyer, E. Y. Spenser, and G. F. Wright, Can. J. Res., 24B, 200 (1946).
67. G. Boche and J. Bigacke, Tetrahedron Lett., 25, 955 (1984).
68. M. R. Winkle, J. M. Lansinger, and R. C. Ronald, J. Chem. Soc. Chem. Comm., 87 (1980).

CHAPTER 2

REGIOSPECIFIC FLUORINATION OF ARYL ANIONS WITH XENON DIFLUORIDE

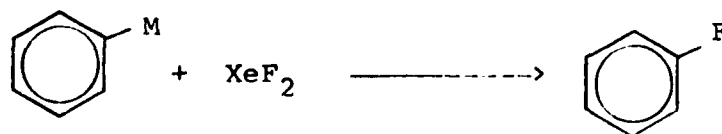
Walter B. Avila and Kevin A. Lang

ABSTRACT

This is a continuation of the investigation of xenon difluoride with organometallics. The investigation has been extended to the model system 4-bromoanisole. The compound 4-trimethylsilylanisole was prepared in 96% yield from 4-bromoanisole and will be investigated for possible utility as an intermediate for the synthesis of fluoroaromatics.

Background/Results/Discussion

This is a continuing effort to develop a new synthesis of fluoromatics by reaction of xenon difluoride with organometallics.

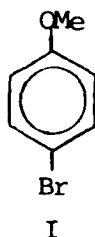


M = Li, MgX, etc.

Additional results on the investigation of the phenyllithium system under a variety of solvent and temperature conditions did not give any of the desired fluorobenzene.

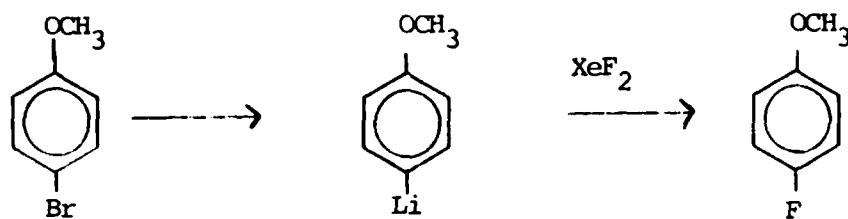
The initial investigation of alternate Lewis acid catalysts was started. The boron trifluoride etherate was replaced by aluminum

fluoride. Several reactions were run in pentane at temperatures from -78°C to room temperature. The results again showed none of the desired fluorobenzene as product (GC/mass spec analysis). The difficulties in separating fluorobenzene, benzene, and the reaction solvents by the GC/mass spectral analysis procedure prompted our change to the model system 4-bromoanisole (I).



This compound, when converted to its organolithium analog would give rise to 4-fluoroanisole upon reaction with xenon difluoride. The physical properties of 4-fluoroanisole (bp 157°C) allow for easy work-up and the removal of the reaction solvents which have previously interfered with the GC/mass spectral analysis. The reaction of I with xenon difluoride is shown in Table I. Again, no fluorinated products were observed. It is interesting to note that 4-bromoanisole was recovered as the major product with minor amounts of fluorobromo- and dibromoanisole as by-products. The mechanistic implications of the formation of these undesired products is currently being investigated.

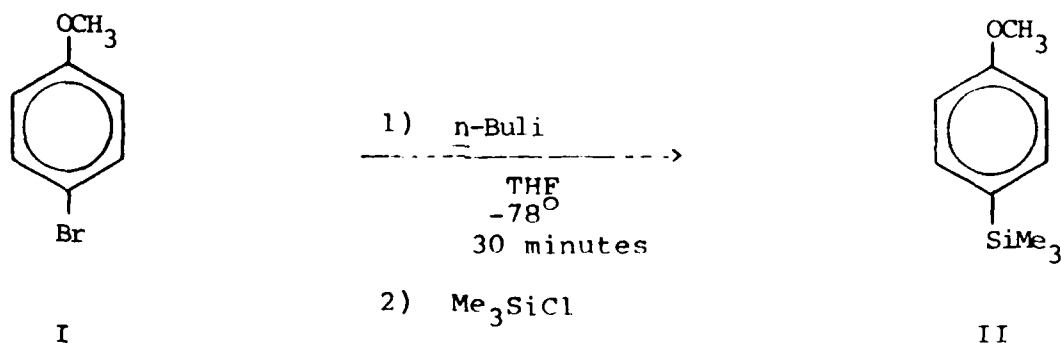
TABLE I
Reaction of 4-Bromoanisole with Xenon Difluoride



I

Entry	Solvent	Rxn Conditions, Temp (°C)	Complexing Agent	Comments
1	Et ₂ O	-78 to RT overnight	--	4-bromoanisole major product, trace of dibromo & fluorobromo product
2	pentane	-78 2 1/2 hrs	BF ₃ ·Et ₂ O	no product, XeF ₂ unreacted
3	Et ₂ O	-78, 3 1/2 hrs	BF ₃ ·Et ₂ O	no product

In an effort to develop an alternate pathway to fluoroaromatics and still take advantage of the synthetic utility of organolithium compounds the reaction scope was expanded to include silicon substituted aromatics. Organosilicon chemistry is well documented.^{2,3,4} The electrophile-induced desilylation or ipso-desilylation of aromatic compounds is one such area. Compound I was converted to 4-trimethylsilylanisole (II) by reaction with n-butyllithium and trimethylsilylchloride in 96% yield.



Compound II was then used as a model system in reactions with xenon difluoride. The initial results utilizing II will be reported on in future publications.

Conclusions

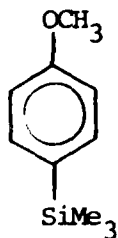
The 4-bromoanisole system has not proved promising for the fluorination reactions. Efforts will be shifted to the 4-trimethylsilylanisole system which offers greater potential. Possible extensions to other organometallics and enolate anions will also be investigated.

EXPERIMENTAL PROCEDURES

General

General experimental information is contained in Reference 1.

4-Trimethylsilylanisole



4-Bromoanisole (aldrich, 2.299, 12.2 m/mol) was placed in a 35 ml flask with a stir pea and the flask was purged with argon. THF (10 ml) was

added and the contents were cooled to -78°C with a dry ice/acetone bath. *n*-Butyllithium (aldrich, 7.75 ml, 1.58 M in hexane) was added dropwise with stirring and a white precipitate formed. The reaction was stirred at -78°C for 45 minutes then trimethylsilylchloride (aldrich, 1.63 ml, 12.84 mmol) was added. The reaction was allowed to stir overnight and gradually warm to room temperature. An aqueous work-up was followed by an ether extraction. The organic phase was dried with anhydrous magnesium sulfate, filtered, and concentrated to give 3.066 g of II as a colorless liquid. Purification by kugelrohr distillation (bp 82.9-85.2 at 0.34 torr) gave 2.12 g of II as a colorless liquid: pmr (CDCl_3 ; δ .240 (s, 9H), 3.77 (s, 3H), 6.89 (d, 2H), 7.44 (d, 2H); ir (film) 1600, 1505, 1280, 1250, 850, 835 cm^{-1} ; m/e 180, 165, 135.

Acknowledgement

The authors wish to thank Mr. Lloyd Pflug, FJSRL, for the GC/mass spectral and NMR analyses, without which this work would not have been possible.

References

1. The initial information is contained in USAFA-TR-84-6, March 1984.
2. Robert West and Thomas J. Barton, J. Chem Ed, 57, 165 (1980); ibid 57, 334 (1980).
3. E. Culvin, Silicon in Organic Synthesis, Butterworth and Co. Ltd., Boston, MA, 1981.
4. Silicon Compounds Register & Review, Petrarch Systems, Inc., Bristol, PA, Catalog S-5.

CHAPTER 3

CORRELATION OF σ^{13} CONSTANTS WITH NMR CHEMICAL SHIFTS IN FLUORINE, PHOSPHORUS, AND NITROGEN-CONTAINING STYRENE DERIVATIVES

Charles N. Robinson

ABSTRACT

The P-31 chemical shifts of two series of compounds (m & p-substituted triethyl d-phosphonocinnamates and diethyl d-phosphonocinnamitriles) have been determined and the chemical shifts of the phosphorous atoms have been plotted against σ^{13} values giving correlation coefficients of -0.991 and -0.989, respectively. Thus the phosphonate is similar to the carbethoxy group in giving an excellent correlation (and a negative slope) when attached to the β -carbon of the styrene moiety. The F-19 chemical shifts of a series of m and p-substituted ethyl d-fluorocinnamates were also determined and the chemical shifts of the fluorine atoms plotted against σ^{13} values. In this case the correlation coefficient is also quite good (+0.981). It is suggested that the positive slope in this case may be a result of the fact that unlike the CO_2Et , CN , PO_3Et , and other groups attached at this position the fluorine atom has unshared pairs of electrons and is capable of resonance stabilization of a positive charge at the adjacent (β) carbon.

INTRODUCTION

The correlation of substituent effects and ^{13}C chemical shifts has received considerable attention. Although the possible signifi-

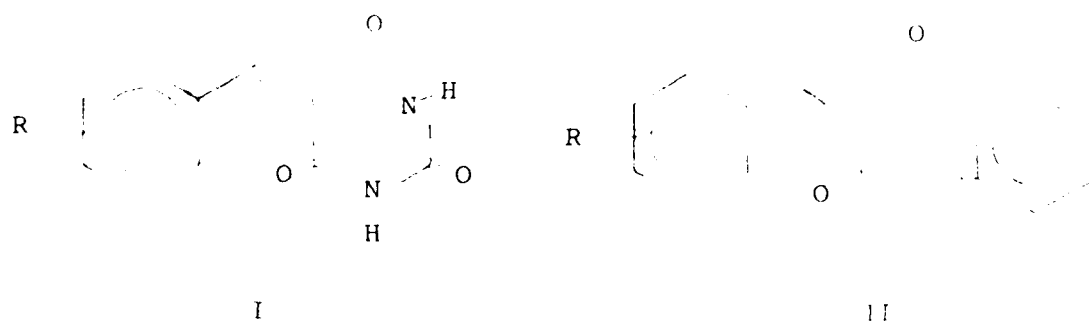
cance of a variety of influences has been pointed out (1), it is apparent that charge densities can be the primary determinant of chemical shift differences in series of compounds in which other factors are maintained fairly uniform throughout. Perhaps because this latter requirement was not met, earlier calculations (2-4) did not lead to entirely successful correlations. Better results have been reported, however, for carbon atoms in π -electron systems, including monosubstituted benzenes (5), chalcones (6), and a variety of arylcarbenium ions (7,8).

Additionally, several workers have explored the anticipated relationship between Hammett σ values and chemical shift, and excellent correlations have been observed when Brown and Okamoto σ^+ values (9) are used. These have been sufficiently precise to lead to the suggestions that σ^+ constants can be determined in this way. Both Posner and Hall (10) and Cornelis et al. (11) have reported such constants based on the shift of the carbon atom attached to the cyano groups in substituted benzylidene malononitriles. Bromilow and Brownlee (12) have suggested the use of benzonitriles for these determinations.

The search for Hammett correlations has brought to light an apparent anomaly. In general, the direction of substituent-caused chemical shifts is logically predicted, with electron donors increasing the shielding at other centers and electron acceptors decreasing it. Bromilow and Brownlee (12) first called attention to a "reverse" correlation found in the m- and p-substituted

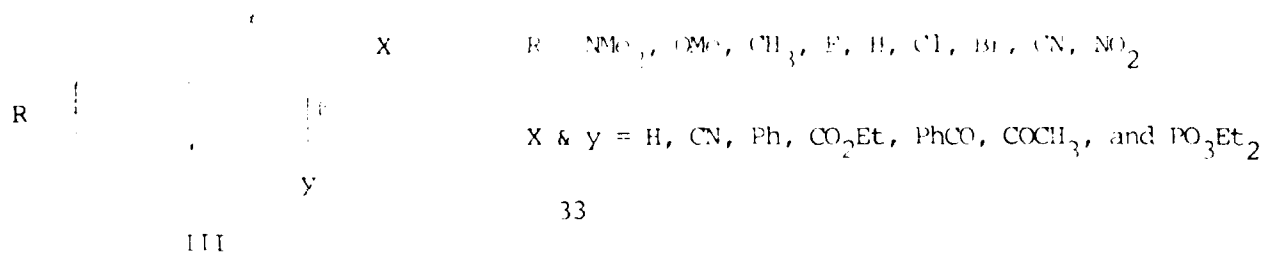
benzonitriles. In both series the resonance of the carbon atom of the cyano group moved down field as the electron donating ability of the substituent increased, while the opposite was true for the ring carbon to which the cyano group was attached.

We first reported (13) that reverse correlations could also be observed between Brown and Okamoto σ^+ values and the chemical shifts of certain carbonyl groups attached to the β -carbon of the styrene moiety in two series of compounds, the 5-arylidenebarbituric acids, I, and 2-arylidene-1,3-indanediones, II. Correlation coefficients



for these carbonyl groups ranged from -0.985 to -0.994. These are especially good correlations in view of the low slopes of the lines. Relative slopes indicate that the carbonyl carbons are an order of magnitude less susceptible to changes in electron density than the β -carbons of the styrene moiety.

In a later article (14) we reported chemical shift data for 12 series of p-substituted styrenes, III, and pointed out that the correlation coefficients for the plot of σ^+ values vs the chemical

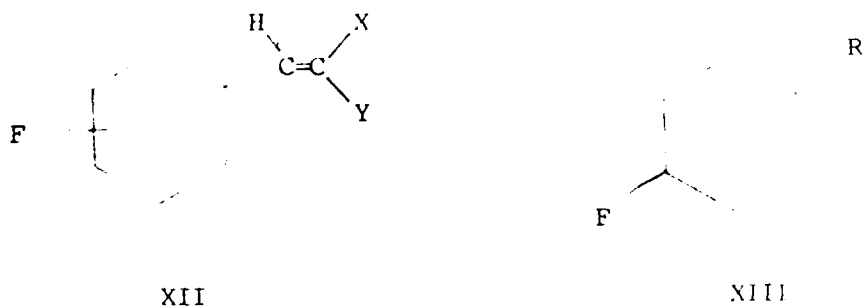


the substituent, $-CH=CXY$, while the δ_{p-F} and the δ_{o-F} are attributable to both inductive and resonance effects, the differences mentioned above should give at least a crude estimate of the relative electron withdrawing/donating resonance interactions of the $-CH=CXY$ substituent. The data presented in Table IV shows that although the correlation between calculated σ^{13} values for the p-nitro substituent and the $\delta_{m-F} - \delta_{p-F}$ is far from perfect, it is good enough to indicate that the resonance interaction or electron-demand of the $-CH=CXY$ group is an important factor in variations of σ^{13} values at the para position. In the case of ortho-substituted compounds, the data would indicate that the $-CH=CXY$ groups are electron donating. This is not a reasonable result and it appears that the proximity of the two groups is such as to make other factors (steric effects) overshadow the resonance interactions we were trying to observe.

Attempts to run N-15 chemical shift studies on compounds of type VIII and IX have been unsuccessful.

It is also not yet apparent whether Graph III consists of a single line as shown or of two lines, one for the electron donating groups due to the inductive stabilization of a negative charge on the β -carbon, X, and another for the electron withdrawing groups involving the resonance stabilization of a positive charge on the β -carbon of the styrene moiety, XI. It is obvious that more data points at both ends of this line are needed. The synthesis of the necessary compounds for clarifying this point is being carried out by Gregory E. Stablein, one of my graduate students at Memphis State University.

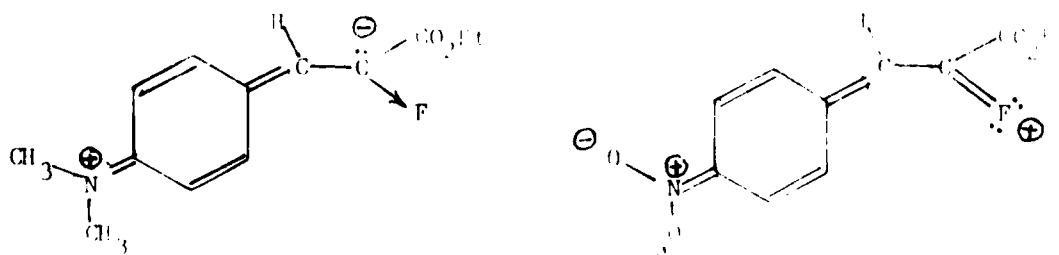
A second F-19 study is being carried out on o-, m-, and p-fluoro derivatives of β -substituted styrene molecules, XII, in order to determine whether the differences in F-19 shifts, $\delta_{m-F} - \delta_{p-F}$

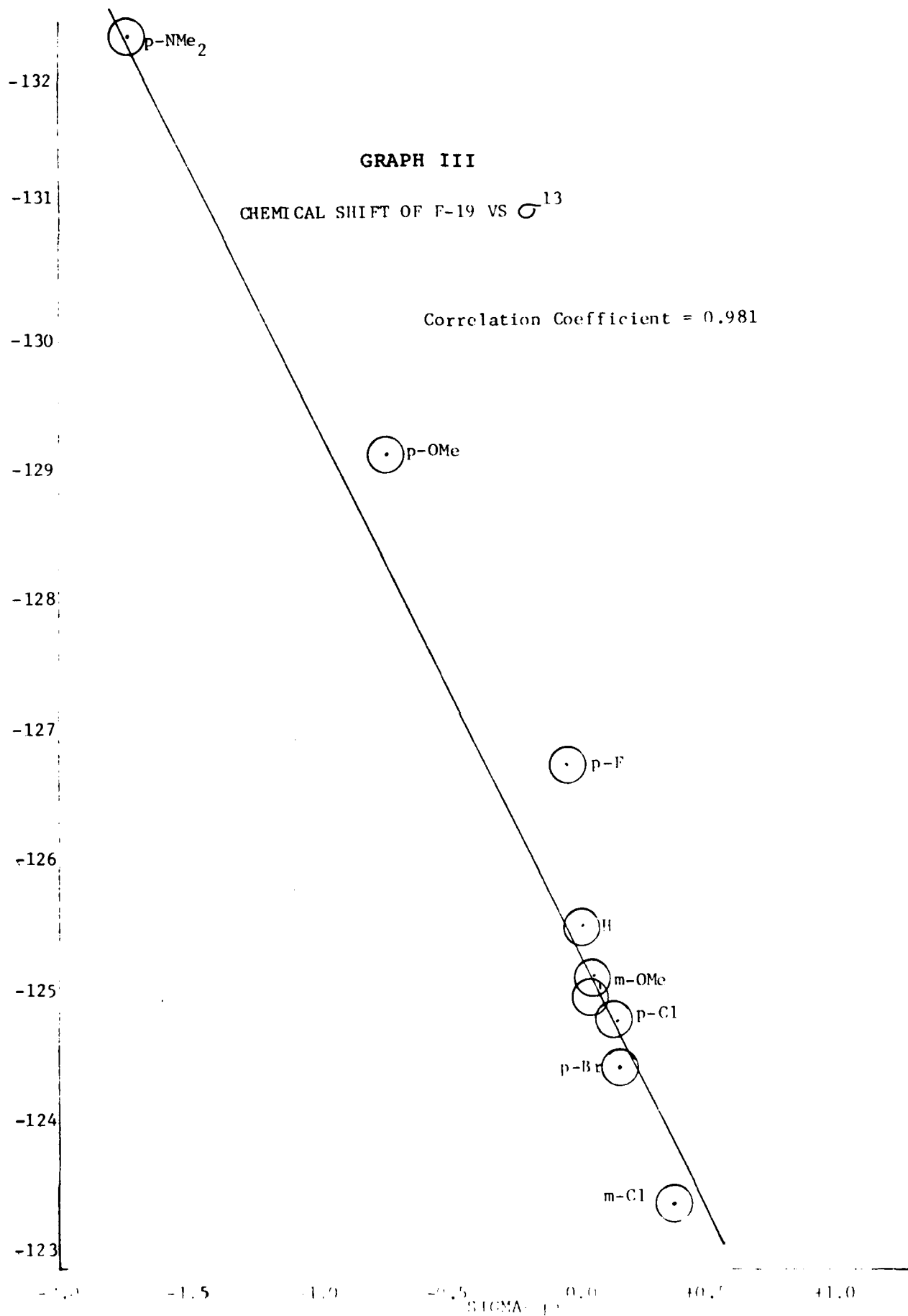


and $\delta_{m-F} - \delta_{o-F}$, can be used to account for differences in individually calculated σ^{13} values, particularly for strong electron withdrawing groups on the aromatic ring. Taft (20) has used a similar method for calculating σ_R^o values of R- groups in compounds of type XIII. Since the δ_{m-F} value is due only to the inductive effect of

the P-31 chemical shifts of several of the Z-isomers of these compounds. These were not prepared separately; they were observed as impurities in the E-isomers. The existence of both the cis and trans isomers had not been previously suspected; elemental analysis, of course, would not reveal the presence of both isomers and the amount of Z-isomer present was so small that it was not observed in either proton or C-13 NMR spectra. It is also apparent that the same $\delta_P - \sigma^{13}$ correlation can be expected for this series.

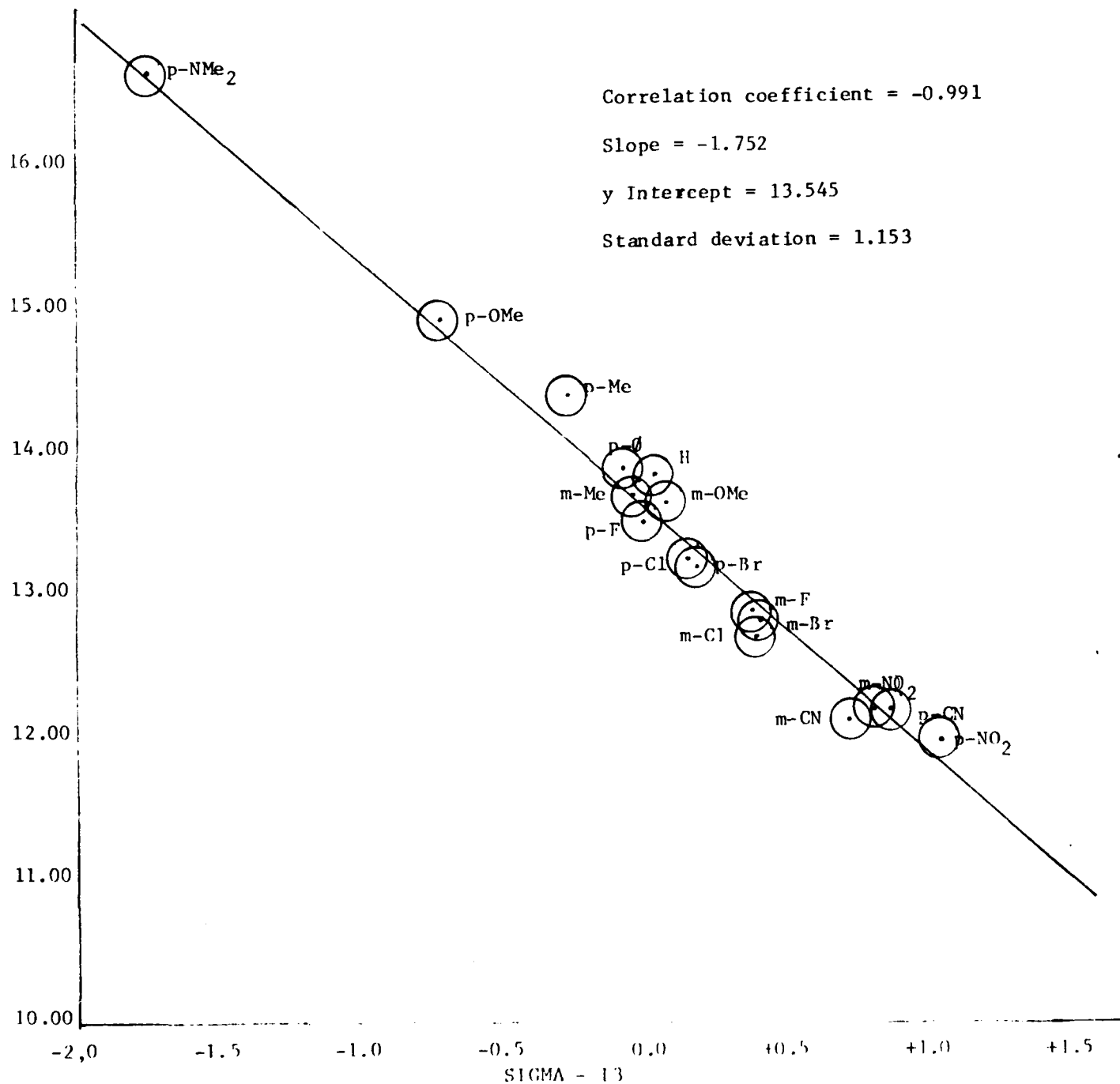
The F-19 chemical shift data for ethyl d-fluorocinnamates, VII, is presented in Table III and Graph 3. Only 8 members of this series have been prepared to date, but the results are somewhat surprising. First, although a good correlation coefficient of +0.981 is obtained when δ_F is plotted against σ^{13} , the slope is positive as opposed to the negative slopes observed for the phosphorus and carbon atoms in this position. It is suggested that the fluorine atom, like the PO_3Et_2 , CN, CO_2Et , and keto groups, can act as an electron withdrawing group by inductive effect, but that it can also act as an electron donating group via resonance interaction of the unshared electron pairs on the fluorine atom which the other groups lack.





GRAPH II

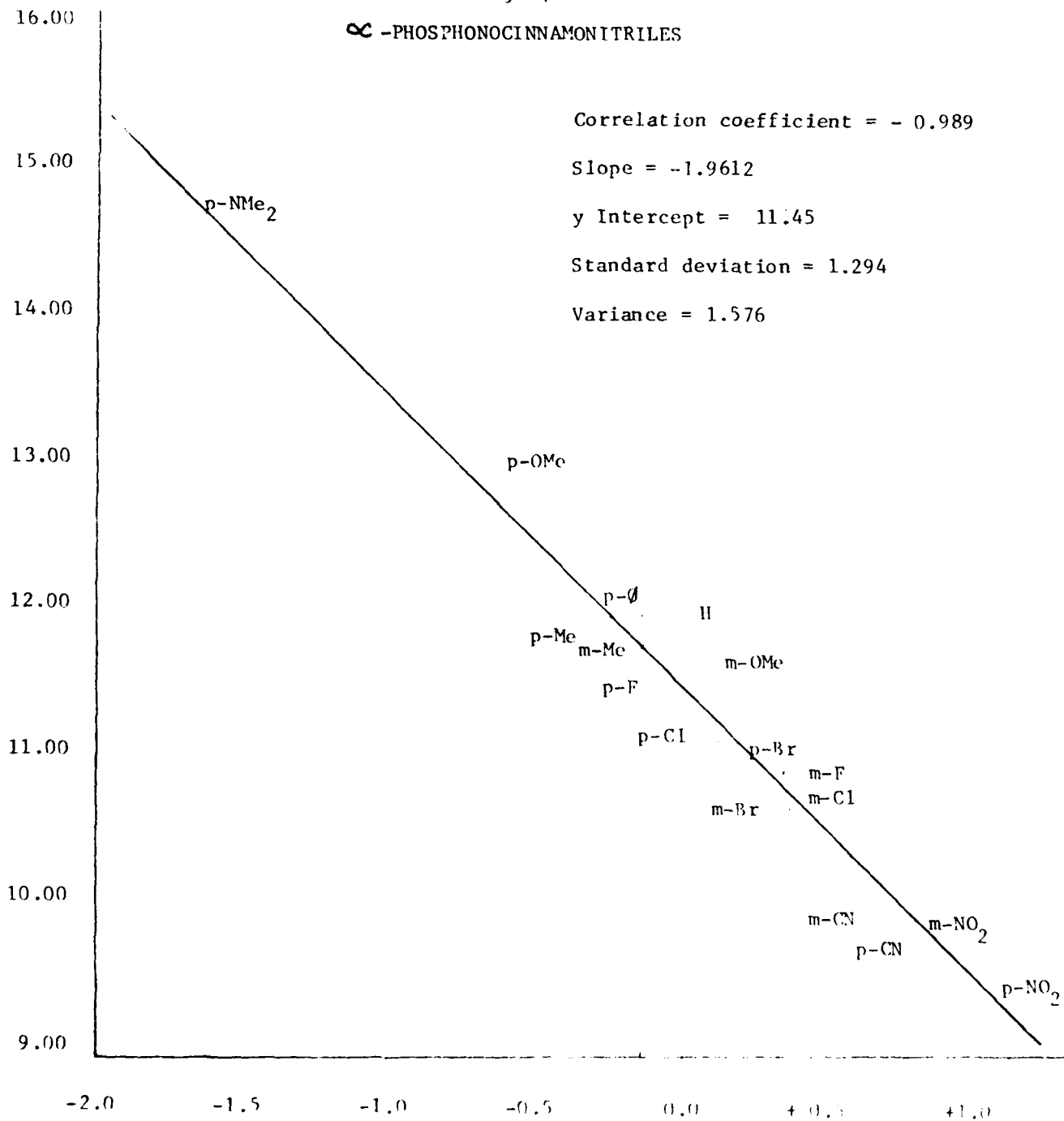
CHEMICAL SHIFT ($\delta_P - \delta_{H_3PO_4}$) OF P-31 VS σ^{13} OF
TRIETHYL α -PHOSPHONOCINNAMATES



GRAPH I

CHEMICAL SHIFT ($\delta_P - \delta_{H_3PO_4}$) OF P-31 VS σ^{13} OF DIETHYL

α -PHOSPHONOCINNAMONITRILES



SIEMENS-13

TABLE III

Chemical Shifts of Heteroatoms in Diethyl d-Phosphocinnamitriles, Triethyl d-Phosphocinnamates, and Ethyl d-Fluorocinnamates (solvent = CDCl₃).

Substituent	δ -p ^a	δ -p ^b	δ -p ^c	δ -F ^d
p-NMe ₂	14.673	16.598		-132.37
p-OMe	12.986	14.861		-129.13
p-Me	11.814	14.255		
p-O	11.896	13.865		
m-Me	11.676	13.623		
p-F	11.447	13.434	11.078	-126.79
H	11.935	13.810	11.361	-125.54
o-Me	11.603	13.596	11.348	-125.06
p-Cl	11.212	13.178	10.850	-124.82
p-Br	11.097	13.138		-124.44
m-F	10.844	12.815	10.540	
m-Cl	10.657	12.761	10.567	-123.42
m-Br	10.524	12.788		
m-CN	9.855	12.142	10.002	
m-NO ₂	9.813	12.198		
p-CN	9.717	12.182		
p-NO ₂	9.476	11.994		

^aP-31 Chemical shifts in diethyl d-phosphocinnamitriles, down field from H₃PO₄ (ext). ^bP-31 Chemical shifts in E-triethyl d-phosphocinnamates, down field from H₃PO₄ (ext). ^cP-31 Chemical shifts in Z-triethyl d-phosphocinnamates, down field from H₃PO₄ (ext). ^dF-19 Chemical shifts in Ethyl d-fluorocinnamates, up field from CFCl₃ (int).

TABLE II

PARAMETERS FOR P-31

ACCUM:

POINT = 8192
 SAMPO = 8192
 TIMES = 16
 DUMMY = 0
 FREQU = 2000Hz
 FILTR = 1000Hz
 DELAY = 0.4500 mS
 OBSET = 62.8000
 ACQTM = 2.0480
 PD = 5.000

PULSE

PULCO = SINGLE
 PUMOD = 1
 PW1** = 19.0000
 PW2** = 20.0000
 P1*** = 1
 PD*** = 5.000
 LOOP: = 1
 HS*** = /OFF
 SPOIL = 1.000
 PREDL = 200.0000
 DEADT = 50.000
 INIWT = 1.0000

CONST:

OBFRQ = 36.21
 IRFRO = 90.00
 IRSET = 54.2000
 LN
 IRPOW = 63
 TEMP = 30.0

 IRMOD = COM = 1 =
 DECOUPLED
 = NON for
 coupling
 NOISE = 2.5Hz

PARAMETERS FOR F - 19

ACCUM:

POINT = 16384
 SAMPO = 16384
 TIMES = 16
 DUMMY = 0
 FREQU = 16000 Hz
 FILTR = 8000 Hz
 DELAY = 12.5000
 OBSET = 57.3400KHz
 ACQTM = 0.512
 PD = 1.0000

PULSE

PULCO = SINGLE
 PUMOD = 1
 PW1** = 10.0000
 PW2** = 80.0000
 P1*** = 1.0000
 PD*** = 1.0000
 LOOP* = 1
 HS*** = /OFF
 SPOIL = 0.50000
 PREDL = 200.000
 DEADT = 50.0000
 INIWT = 1.0000

CONST:

OBFREQ = 84.25 MHz
 IRFREQ = 90.00 MHz
 IRSET = 54.20000
 LN
 IRPOW = 63
 TEMP = 30.0

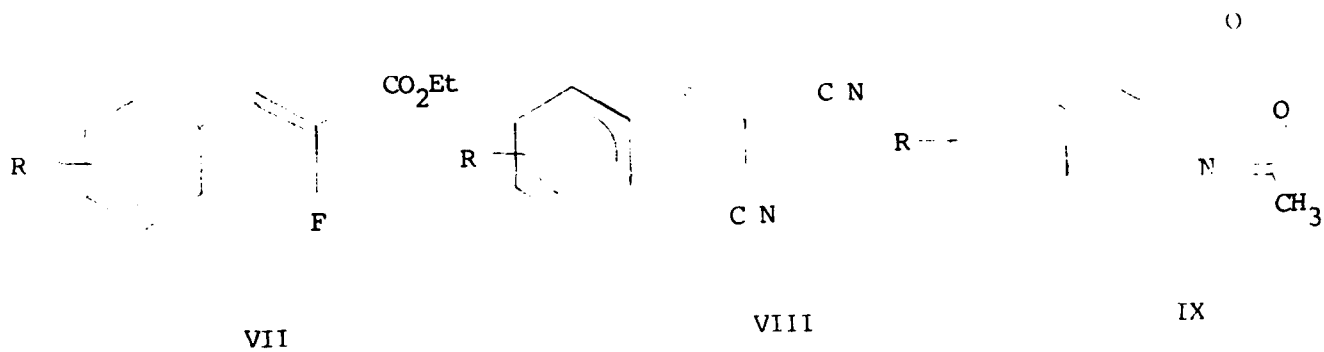
 IRMOD = NON = 0
 Coupled
 NOISE = 2.5 KHz

EXPERIMENTAL RESULTS

Both P-31 and F-19 spectra were run on the FJSRL instrument, a JNM FX90Q FT NMR Spectrometer. Characteristic parameters for both P-31 and F-19 are listed in Table II. The chemical shifts for both the phosphorus and fluorine compounds are presented in Table III.

As can be seen from both Table III and Graph I, the chemical shift of the p-dimethylamino derivative of diethyl d-phosphonocinnamionitrile is considerably different from that of the p-methoxy derivative. There is nothing anomalous about that compound and, in fact, the series gives an excellent P-31 chemical shift- σ^{13} correlation (coefficient = -0.989). The results from the cinnamate esters, Graph II, bear out these results (correlation coefficient = -0.991) and it is apparent that the phosphorus atom chemical shift data is similar to the carbon atoms of ester groups attached to the β -position of styrene type molecules (i.e., good correlations, negative slopes, and low slopes although it should be observed that the slopes of the P-31 plot are about twice those of malonate esters, indicating that the phosphorus atom is more susceptible to changes in electron density due to substituent effects than is the carbonyl group in this position). Table III also lists

Several other series of compounds, VII - IX, were also to be



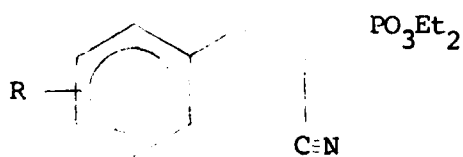
examined for F-19 or N-15 correlations with σ^{13} .

TABLE I. Substituent Constants.^a

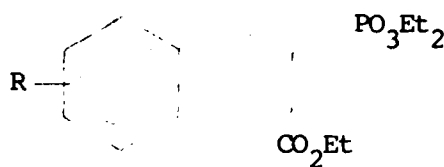
Substituent	σ	σ^+	σ^-	σ^{13}
p-N(Me) ₂	-0.83	-1.7	0.83	-1.75
p-OMe	-0.27	-0.78	-0.27	-0.74 \pm 0.03
p-Me	-0.17	-0.31	-0.17	-0.30 \pm 0.03
p-Ph	-0.01	-0.18	-0.01	-0.10 \pm 0.03
p-F	0.06	-0.07	0.06	-0.05 \pm 0.02
H	0.00	0.00	0.00	0.00
p-Cl	0.23	0.11	0.23	0.13 \pm 0.05
p-Br	0.23	0.15	0.23	0.15 \pm 0.05
p-CN	0.66	0.66	0.90	0.85 \pm 0.15
p-NO ₂	0.78	0.78	1.24	1.01 \pm 0.19
m-Me	-0.07	-0.07	-0.07	-0.07 \pm 0.01
m-OMe	0.12	0.12	0.12	0.05 \pm 0.03
m-F	0.34	0.34	0.34	0.35 \pm 0.05
m-Cl	0.37	0.37	0.37	0.36 \pm 0.05
m-Br	0.39	0.39	0.39	0.36 \pm 0.06
m-CN	0.56	0.56	0.56	0.69 \pm 0.10
m-NO ₂	0.71	0.71	0.71	0.79 \pm 0.12

^a σ , σ^+ , and σ^- values were taken from Ref. 9.

examine the possibility of a similar correlation with other atoms. One series of compounds, the diethyl α -phosphonocinnamitriles V, had been prepared for our C-13 work; this series of compounds was sent to Randolph Bright at the University of Vermont where P-13 NMR facilities were available. The results of this study were somewhat confusing; an excellent correlation was observed for δ_p vs δ^{13} for all substituents except the dimethylamino group for which the chemical shift was almost identical to that of the methoxy group (19). The first problem I wished to address, therefore, was a repetition of this work to be certain that this shift of the dimethylamino group was not in error. A second series of compounds, the triethyl α -phosphonocinnamates, VI, was also prepared so that, if the dimethylamino group shift was anomalous, I would have another example for comparison.



V



VI

from the compounds we have examined (I-IV). The latter approach (use of a combination of σ^+ and σ^-) was suggested by Krabbenhoft (17), who found that the use of the σ^- value for p-nitro, along with the σ^+ value for other substituents, was needed to obtain an adequate correlation in the β,β -dichlorostyrene series.

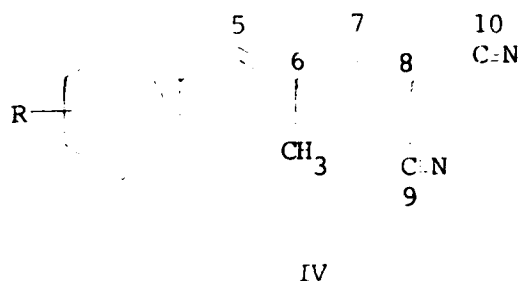
In view of the use of NMR data to calculate σ^+ values, the wide variety of compounds which could be used to make these calculations (thus leading to a variety of σ^+ values for the same substituent), and the confusion over which type of substituent constant to use (σ , σ^+ , σ^- , or some combination thereof), we have proposed the use of a new σ^{13} scale that is not tied to the σ^+ scale in any way except by a scaling factor. The σ^{13} scale is defined in Eq. [1], in which a is a factor introduced to scale the value for the p-dimethylamine group to -1.75,

$$\sigma^{13} = a (\delta_x - \delta_H) \quad [1]$$

so that σ^{13} values would be in the same general range as other σ scales and so that the values determined for each set of compounds would be similarly scaled. In a more recent article (18) we have selected 17 series of substituted styrenes on which to base the evaluation of σ^{13} constants and have extended these constants to meta as well as para substituents. A comparison of σ^{13} values with other relevant substituent constants is shown in Table I.

In view of the excellent substituent effect correlations observed with carbon-13 NMR chemical shifts we wished next to

shifts of the β -carbons are invariably excellent (+0.9909 to +0.9986) and that reverse correlations are by no means unusual and are consistent with charge density arguments. The vinylogous 1,1-dicyano-3-methyl-4-aryl-1,3-butadienes, IV, were also prepared, and



it was shown that in fact there is a regular alternation of sign in the line slopes at the carbon atoms numbered 5-10 (positive slopes at C6 and C8 and negative at C5,7,9&10). This is in line with Pople and Gordon's (then startling) finding (15), based on CNDO/2 calculations on fluoroalkanes, that if a substituent causes that atom to which it is attached to be depleted of electron density, the adjacent attached atom will become somewhat electron rich. Fliszar (16) applied a variety of calculational approaches to the study of the alkanes and concluded that "a positive site is best favored when embedded in negative surroundings."

It should be pointed out that the use of σ or a combination of σ^+ and σ^- substituent constants provided generally less satisfactory results (than σ^+ alone) when correlated with chemical shift data

TABLE IV

COMPARISON OF F-19 CHEMICAL SHIFTS IN ORTHO, META, AND PARA SUBSTITUTED STYRENES

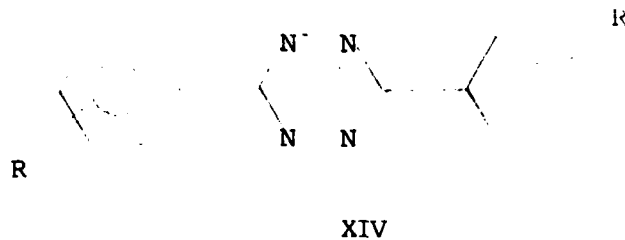
β -Substituents	δ_{o-F}	δ_{m-F}	δ_{p-F}	$\delta_{m-F} - \delta_{o-F}$	$\delta_{m-F} - \delta_{p-F}$	$\sigma_{p-NO_2}^{13}$
CO- <u>t</u> -Bu/H	-114.3	-113.1	-110.2	+1.2	-2.9	1.36
CO ₂ Et/H	-115.0	-113.0	-110.2	+2.0	-2.8	1.28
1-tetralone	-112.5	-113.2	-112.2	-0.7	-1.0	1.25
1-indanone	-113.5	-112.7	-110.2	+0.8	-2.5	1.25
\emptyset CO/H	-114.0	-112.9	-109.5	+1.1	-3.4	1.22
<u>E</u> -CN/H	-	-112.2	-108.3	-	-3.9	1.19
<u>Z</u> -H/CN	-	-112.1	-108.2	-	-3.9	1.08
\emptyset /CN	-115.0	-112.2	-108.8	+2.8	-3.4	1.03
CO-CH ₃ /CO- \emptyset	-113.4	-112.3	-108.8	+1.1	-3.5	1.05
CO ₂ Et/CO ₂ Et	-113.3	-112.6	-109.1	+0.7	-3.5	0.96
PO ₃ Et ₂ /CO ₂ Et	-113.1	-112.6	-109.3	+0.5	-3.3	0.96
CO ₂ Et/Ac (<u>E</u>)	-	-114.2	-109.2	-	-5.0	0.93
Ac/CO ₂ Et (<u>Z</u>)	-	-113.0	-108.8	-	-4.2	0.82
CO ₂ Et/CN	-112.3	-111.1	-103.6	+1.2	-7.5	0.85
PO ₃ Et ₂ /CN	-	-111.1	-104.1	-	-7.0	0.81
CN/CN	-111.5	-110.0	-100.7	-	-9.3	0.80
\emptyset CO/CN	-	-111.0	-103.3	-	-7.7	0.78

The natural occurrence of the N-15 isotope is so low (0.37%) that NMR studies using it are quite difficult. However, work is continuing to find proper parameters for studying these compounds. It may be necessary to resynthesize these compounds using isotopically enriched nitrogen-15 before this study can be completed.

Finally, although it was not planned as a part of this work, Mr. Lloyd Pflug has run mass spectra on the 109 compounds used in this NMR study. This data has not yet been analyzed and is too extensive to present here. However, it is anticipated that interesting conclusions can be drawn on the effect of substituent groups on the mass spectra of styrene types of molecules.

FUTURE WORK

The proposed P-31 work has been completed. However, it will be necessary to synthesize and run F-19 spectra on several other examples (9 are planned) of the ethyl d-fluorocinnamates before any final conclusions can be drawn. Work will also continue on the proposed N-15 studies. It was also anticipated that a series of substituted diphenyltetrazines, XIV, would be prepared by senior



research students; however, these compounds were not prepared. I would like to have these compounds prepared for C-13 and N-15 studies in order to determine whether or not chemical shift data on the tetrazine ring atoms can be correlated with calculated electron densities. These compounds are of interest because of their potential use as energetic materials.

ACKNOWLEDGEMENTS

The author would like to express his appreciation to Mr. Lloyd Pflug and the other personnel at FJSRL for their technical help and for financial support of this work.

REFERENCES

1. G.E. Maciel, in "Topics in Carbon-13 NMR Spectroscopy" (G.C. Levy, Ed.), Vol. 1, pp. 53-78, Wiley-Interscience, New York, 1974.
2. J.A. Pople and G.A. Segal, J. Chem Phys. **44**, 3289 (1966).
3. J.M. Sichel and A. Whitehead, Theor. Chim. Acta **5**, 35 (1966).
4. P.D. Ellis, G.E. Maciel, and J.W. McIver, Jr., J. Am. Chem. Soc. **94**, 4069 (1972).
5. G.L. Nelson, G.C. Levy, and J.D. Cargioli, J. Am. Chem. Soc. **94**, 3089 (1972).
6. E. Solcaniova, S. Toma, and S. Gronowitz, Org. Magn. Reson. **8**, 439 (1976).
7. D.A. Forsyth, R.J. Spear, and G.A. Olah, J. Am. Chem. Soc. **98**, 2512 (1976).
8. D.A. Forsyth and G.A. Olah, J. Am. Chem. Soc. **98**, 2512 (1976).
9. R. Fuchs and E.S. Lewis, "Investigation of Rates of Mechanism of Reactions," Part I, 3rd Ed., in "Techniques of Chemistry" (A. Weissberger, Ed.), Vol. VI, pp. 777-824, Wiley-Interscience, New York, 1974, gives a recent critical review of the various Hammett constants.
10. T.B. Posner and C.D. Hall, J. Chem. Soc. Perkin Trans. **2**, 729 (1976).
11. A. Cornelis, S. Lambert, and P. Laszlo, J. Org. Chem. **42**, 381 (1977).
12. J. Bromilow and R.T.C. Brownlee, Tetrahedron Lett., 2113 (1975).
13. C.N. Robinson and C.C. Irving, Jr., J. Heterocycl. Chem. **16**, 921 (1979).
14. Charles N. Robinson, Carl D. Slater, John S. Covington III, Chung R. Chang, Louise S. Dewey, John M. Franceschini, James L. Fritzsche, John E. Hamilton, Charles C. Irving, Jr., John M. Morris, Dale W. Norris, Larry E. Rodman, Vernon I. Smith, Gregory E. Staublein, and Forrest C. Ward, J. Magnetic Resonance, **41**, 293 (1980).
15. J.A. Pople and M. Gordon, J. Am. Chem. Soc., **89**, 4253 (1967).
16. S. Fliszar, J. Am. Chem. Soc., **94**, 7386 (1972).

17. H.O. Krabbenhoft, J. Org. Chem., 43, 1830 (1978).

18. Charles N. Robinson, Carl D. Slater, Russell Bies, David W. Bryan, Kimun Chang, Andy W. Hill, William H. Moore, Jr., Teresa G. Otey, Mary L. Poppelreiter, John R. Reisser, Gregory E. Stablein, Vayden P. Waddy, III, William O. Wilkinson, and William A. Wray, Submitted to J. Org. Chem., January, 1984.

19. Charles N. Robinson and Randolph Bright, unpublished results.

20. Robert W. Taft, Elton Price, Irwin R. Fox, Irwin C. Lewis, K.K. Anderson, and George T. Davis, J. Am. Chem. Soc., 85, 3146 (1963).

CHAPTER 4

PHOTODEGRADATION OF RIBOFLAVIN

Dennis J. Fife and Gary M. Gfeller

ABSTRACT

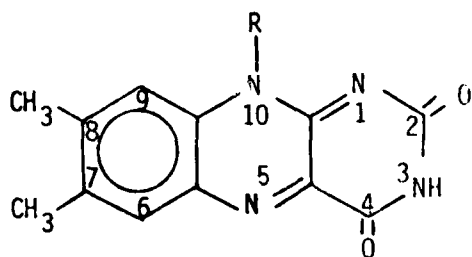
Many mechanisms proposed for the photochemical transformations that take place in the photolysis of riboflavin have been eliminated, a number have survived but remain inconclusive. None of the mechanisms have been satisfactory in explaining all of the experimental observations. The accepted view at present is that the photoexcited isoalloxazine ring system undergoes intramolecular photoreduction in which the ribityl side chain serves as the hydrogen donor (in the absence of an external reductant). This research involves an effort to determine the details of the hydrogen abstraction process proposed in riboflavin by using lumiflavin as a model. Lumiflavin has similar photochemical properties as riboflavin but with a simplified structure (a methyl group in place of the ribityl side chain). The results of the photolysis of lumiflavin in the presence of EDTA and various alcohols are discussed.

INTRODUCTION

An understanding of the biological functioning of riboflavin (Rf, vitamin B₂) lies in the knowledge of the processes of reversible reduction of the isoalloxazine ring system. One means of carrying out the reduction is by reaction of a photoexcited flavin with a hydrogen atom donor, such as ethylenediamine tetraacetic acid

(EDTA).¹ EDTA has been shown to be an effective hydrogen donor to other photoexcited molecules such as methylene blue, uroporphyrin, and thiazine dyes.²⁻³ Photoexcited riboflavin will also extract a hydrogen intramolecularly in which the ribityl side chain serves as the hydrogen donor.⁴ During oxidation of the side chain, fragmentation may occur to produce several of the photoproducts that have been illustrated in Table I. There is very little evidence to support which positions on the ribityl side chain are responsible for the photoproducts. Kinetic isotope effects have not been shown in substituted riboflavin itself (riboflavin-2'-d, riboflavin-3'-d, or with all the hydroxyl hydrogens substituted with deuterium).⁴ Isoalloxazines with much smaller side chains in the N-10 position have had to be used to show kinetic isotope effects.⁵⁻⁶ King proposed that the reason no kinetic isotope effect was observed in riboflavin is because of the number of available reaction sites on the ribityl side chain.⁴ King suggested that if one takes into account all of the possible positions for hydrogen abstraction excluding the 1' position, and assuming the hydrogens on the hydroxyl groups are not involved (total of five possible positions left on the ribityl side chain) that the range of an observable isotope effect would be 1.10

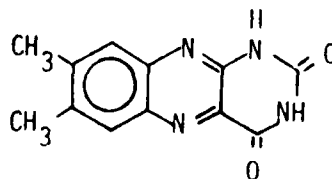
Table I. Structure of Riboflavin and its Photodegradation Products



isoalloxazine ring system

Compound	R
Riboflavin (RF)	$-\text{CH}_2(\text{CHOH})_3-\text{CH}_2\text{OH}$ (D-ribose)
Lumiflavin (LF)	$-\text{CH}_3$
Formylmethylflavin (FMF)	$-\text{CH}_2\text{CHO}$
Carboxymethylflavin (CMF)	$-\text{CH}_2\text{COOH}$
4'-Ketoflavin (4'KF)	$-\text{CH}_2(\text{CHOH})_2-\text{CO}-\text{CH}_2\text{OH}$
2'-Ketoflavin (2'KF)	$-\text{CH}_2-\text{CO}-(\text{CHOH})_2-\text{CH}_2\text{OH}$

Lumichrome (LC)



to 1.46 at most. Thus, it was implied that all five alpha hydrogen are active on the ribityl side chain. If this is the case, then only a product isotope effect would prove of much value in elucidating the mechanism for the main photoproducts of riboflavin photolysis. A definite product isotope effect has been noted between riboflavin, riboflavin,2'-d, riboflavin,3'-d, and riboflavin with a hydroxyl deuterated ribityl side chain.⁷ The product isotope effect suggests that formylmethylflavin is produced from an initial hydrogen abstraction from a hydroxyl hydrogen of the ribityl side chain. This conclusion is in contrast to previous suggestions that the photoexcited isoalloxazine ring does not have the capability to extract a hydroxyl hydrogen.⁵

This research was conducted to experimentally determine the reactivity of a photoexcited isoalloxazine ring with various simple alcohols. Lumiflavin has the exact same ring system as riboflavin but has only a methyl group at the N-10 position. With lumiflavin any interference from intramolecular hydrogen abstraction is eliminated and the intermolecular reactivity of the photoexcited flavin toward several simple alcohols could be determined. This type of analysis coupled with the product isotope effects should help to clarify the positions on the ribityl side chain which are primarily responsible for the different photoproducts.

EXPERIMENTAL

Materials. All chemicals were purchased commercially. Only

spectral grade alcohols were used. Riboflavin was recrystallized from a water-ethanol mixture. Purity of riboflavin was checked by thin layer chromatography using acetic acid-methanol-benzene solvent (1:5:14, v/v). This method is very sensitive to impurities generated by photodegradation.

Apparatus and Spectroscopic Procedures. The photoreactor consisted of a 1000 watt Xenon-Mercury arc lamp at the focal length of a convex quartz lens. The collimated light beam was passed through a distilled water filter to remove heat and then focused on the entrance slit of a monochromator for maximum transmission at 440 nm. The light was then collimated with a convex lens and passed into the photocell. The light intensity through the photocell was $4.8 \pm .1 \times 10^{14}$ quanta $\text{sec}^{-1} \text{cm}^{-2}$ with a band width of approximately 10 nm. The photolysis cell consisted of a round 1.17 cm diameter spectrophotometer cell. The cell was serum-rubber-stoppered with a syringe needle bubbler and a pressure release inverted through the serum stopper. The photocell was flushed with helium for ~10-20 min to remove oxygen. The reaction solution was photolyzed for a few seconds after which the absorbance was measured at 445 nm with a Bausch & Lomb Spectronic 20 Spectrophotometer. Light intensities were determined chemically by riboflavin actinometry¹ and with a thermopile (YSI - Kellering Model 65 Radiometer). The reactions were followed for approximately one half-life. In all cases studied, reoxidation by air completely restored the original absorbance readings at 445 nm.

Quantum Yields. The quantum yield was evaluated both by the initial rate of reduction of the flavin and by the integrated form discussed by Moore and Ireton.⁶ The initial light intensities were determined periodically by riboflavin actinometry and monitored for changes with the thermopile.

Preparation of Solutions. For the reported results, the flavin concentrations were kept in the range of $1.0 \sim 7.0 \times 10^{-5} \text{ M}$ so as to avoid the self-associating region of the flavins. The solutions were diluted to known concentrations determined by absorbance measurements at 445 nm. The flavin solutions were kept in the dark until use and then handled in a dimly lighted room. Stock solutions of EDTA were prepared and then diluted in 25 mL volumetric flasks to the desired EDTA concentrations using flavin solutions and distilled water. The pH of the EDTA solutions were adjusted to pH 7.5.

RESULTS AND DISCUSSION

Figure 1 shows the Stern-Volmer reciprocal plot of quantum yield versus EDTA concentration for lumiflavin. The dashed line shows the literature value for riboflavin.

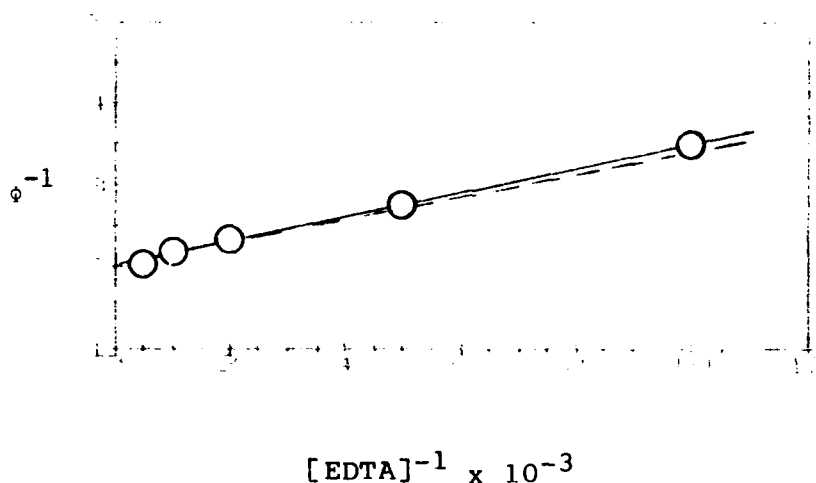


Figure 1. Reciprocal quantum yield of lumiflavin versus reciprocal EDTA concentration at pH 7.5. (— least squares line Int $2.00 \pm .02$, slope $1.48 \pm .04 \times 10^{-4}$; - - - line literature value for riboflavin Int $1.99 \pm .03$ slope $1.4 \pm .1 \times 10^{-4}$).

The quantum yield of reduction of lumiflavin with methanol, 2-propanol, and t-butanol were too low to measure accurately in an alcohol-water mixture, therefore; pure spectral grade alcohols were used. The results are shown in Table II.

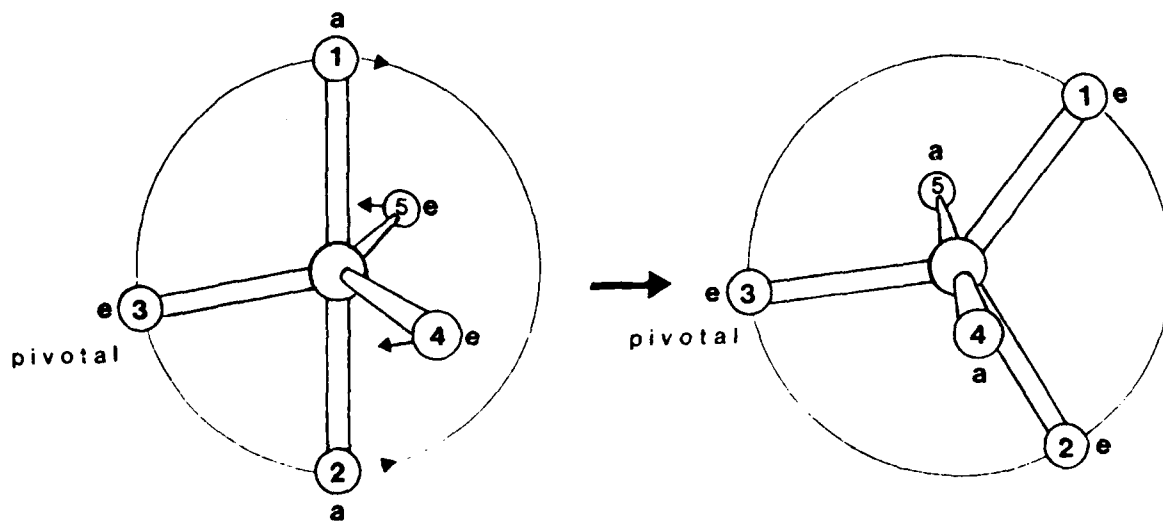
Table II. Quantum Yields for the Photoreduction of Lumiflavin
Using Alcohols as Hydrogen Donors

Alcohol	Quantum Yield
*Water	no measurable reduction
Methanol (25M)	0.005 \pm .002
2-Propanol (13M)	0.05 \pm .01
t-Butanol (11M)	0.06 \pm .01
Glycol (1M) in Methanol	0.05 \pm .01

*shown for comparison

The results of the data available so far in this study clearly shows that lumiflavin can be used as an ideal model for the photoreduction of riboflavin. Lumiflavin does not undergo photodegradation in a water solution since there are no intramolecular hydrogens available. Riboflavin shows a quantum yield of approximately 0.01 in water and approximately 0.2 in alcohols for the disappearance of riboflavin during photolysis. It has been stated that the alcohols shown in Table II do not contribute to the increased reduction of riboflavin since no deuterium isotope effect could be shown.⁶ This could be a mistaken assumption since the solvent alcohol would be in competition with several other intramolecular hydrogen donor sites. The isotope effect from the solvent could be within experimental error. The data in Table II clearly shows that the solvent alcohols must be considered as hydrogen donors. Further

periments to be done are 2-d-2-propanol, and 2-propanol-0-d and butanol-0-d. The isotope effects observed from these compounds could show if the hydrogen abstraction by lumiflavin is taking place at the d-hydrogen to the hydroxyl group or if the hydroxyl hydrogen is abstracted. The relative values of 2-propanol and t-butanol suggest that the hydroxyl group can act as a hydrogen donor. These experiments combined with the previous product isotope effects from substituted riboflavins⁷ should allow some conclusions to be made concerning the positions on the ribityl side chain of riboflavin which are primarily responsible for the photoproducts shown in Table I.



e - equatorial

a - apical

Figure 1. Berry pseudorotation (BPR) of a trigonal bipyramidal geometry showing apical (a) - equatorial (e) exchange.

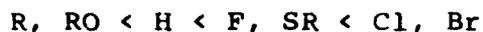
RESULTS AND DISCUSSION

A. Experimental Results

(1) Continuous Variation Study

In Figure 3 EPR signals are shown for 0.5:0.5 aqueous Cu^{2+} metal ion-to-ligand molar ratio and 0.4:0.6 molar ratio. At equal molar concentrations of metal ion and ligand the mono complex predominates in solution. The mono spectrum is a quartet with lines at 3147, 3079, 3008, and 2947 G at 9.0949 GHz. At lower metal ion-to-ligand mole ratio a peak attributable to the bis complex begins to grow in at higher field.

The calculated sequence is exactly that observed in ^1H and ^{29}Si NMR studies of stabilities for trigonal bipyramidal geometry as a function of ligands attached to silicon¹:



The result also correlates well with the interpretation of gas phase kinetics data for nucleophilic attack at silicon that predicts reaction at every collision for ligands having proton affinity above Cl and very slow reaction for ligands below Cl in this sequence.⁶

Thus far we have a model for nucleophilic substitution at silicon in which nucleophiles having proton-affinity greater than Cl^- add to silicon to form stable adducts without activation and nucleophiles with proton affinity less than Cl^- do not form stable adducts. Nucleophilic attack by Cl^- or nucleophiles having smaller proton affinity proceed with inversion of configuration through a SN_2 type transition state analogous to attack at carbon. Conversely, nucleophilic attack on silanes having a leaving group at or below Cl in the proton-affinity sequence proceeds with inversion by a SN_2 reaction having activation energy approximately equal to ΔH for the overall reaction. Substitution for ligands above Cl in the sequence proceed forming a stable TBP intermediate which may undergo intramolecular or intermolecular isomerization.

The proton affinity is a good measure of the enhancement in electronic energy for forming the adduct. This enhancement must be sufficient to overcome the increased core-core repulsions between

TABLE 2

NUCLEOPHILE AFFINITIES FOR $\text{Si}(\text{CH}_3)_3\text{OH}$

REACTION:



Nu^-	Experimental Proton Affinity (kcal/mol)	ΔH°_1 (kcal/mol)	ΔH°_2 (kcal/mol)
CH_3^-	417	-45.7	7.2
OH^-	391	-18.1*	18.1
OCH_3^-	379	-17.0	23.9
F^-	371	-11.7*	19.8
H^-	400	-11.6*	20.3
SH^-	353	-7.2	43.4
Cl^-	333	-4.4	53.5
Br^-	324	unstable	60.2**
I^-	315	unstable	53.5**

*Results obtained by using JANNAF¹⁹ value for heat of formation for Nu^- .

**Values are ΔH for overall reaction.

TABLE 1

NUCLEOPHILE AFFINITIES FOR $\text{Si}(\text{CH}_3)_4$

REACTION: $\text{Nu}^- + \text{Si}(\text{CH}_3)_4 \xrightarrow{\Delta H^\circ} \text{Nu}-\text{Si}(\text{CH}_3)_4$

Nu^-	Experimental Proton Affinity (kcal/mol)	Hardness**	ΔH° (kcal/mol)
CH_3^-	417	soft	
OH^-	391	hard	-7.2*
OCH_3^-	379	hard	-6.3
H^-	400	soft	-1.4*
F^-	371	hard	-0.6*
Cl^-	333	hard	unstable
Br^-	324	borderline	unstable
I^-	315	soft	unstable

*Results obtained by using JANNAF¹⁹ value for heat of formation for Nu^- .

** Hardness classifications by Pearson.²⁰

MNDO predictions of stabilities (ΔH°) for nucleophile adducts to tetramethylsilane are listed in order of decreasing stability in Table 1. There is a good correlation between the gas-phase proton affinity of the nucleophile represented by ΔH for the gas-phase acidity of its conjugate acid and the stability of its adduct, while there is no apparent relationship between the hardness of the nucleophile and the adduct stability. The only exception to this trend with gas-phase acidity is H^- which forms a less stable adduct than expected based on its proton affinity. This exception for the Si-H bond is reasonable because all the other nucleophilic contribute substantial p-character to the bonding molecular orbital for Si-X, which is not possible for hydrogen.

MNDO predictions for stabilities of nucleophile adducts to trimethylsilanol are shown in Table 2. Here again, except for H^- , we see the same trend of adduct stability with nucleophile proton-affinity. The hydroxyl ligand induces additional stability of approximately 11 kcal/mol in the adduct most stable without altering the trend.

transition-state geometries for highly exoergic exchange reactions.¹⁸ (Dewar's group is addressing this problem of overestimated core-core repulsions in a "third-generation" program to follow MNDO¹⁷.)

For the calculations presented here, the first error must be accounted for when a small anionic nucleophile is substantially isolated during nucleophile attack or elimination. However, neither of these errors complicates calculations for intramolecular isomerization. Pseudorotation calculations do not require MNDO to model species having bond distances drastically different from "normal" bond distances for which MNDO is parameterized. We can expect absolute errors in heats of formation for isomerization calculations at least comparable to the average errors advertised for MNDO (± 6 kcal/mol). But more important, relative errors should be small compared to the absolute error. So MNDO is ideally suited to pseudorotation calculations for large species.

RESULTS AND DISCUSSION

Stabilities of Pentacoordinate Adducts

The adduct geometries were all nominally trigonal bipyramidal. The most stable isomer in each case for stable tetramethylsilane adducts placed the nucleophile in an apical position. For trimethylsilanol adducts the most stable isomer placed both the nucleophile and OH in apical positions. Stable adducts were formed without activation.

elements except lithium and neon, and some third row elements.¹⁶

For each reaction path, we chose as a reaction coordinate a bond angle or bond distance that changed appreciably during the reaction. We performed a reaction path calculation by holding the reaction coordinate fixed at a number of selected values while allowing the rest of the molecule to completely optimize. To model pseudorotation either the bond angle between an apical and equatorial ligands or between two equatorial ligands was chosen as reaction coordinate. The pseudorotation profiles produced were relatively insensitive to the particular bond angle chosen, and the apparent activation barriers were even less sensitive. However, a retardation in bond angles other than the reaction coordinate leads to a small hysteresis effect. All stationary points on the potential surface were optimized using procedures supplied with the MOPAC package of programs. There are two known situations for which MNDO exhibits large systematic errors. First, MNDO overpredicts heats of formation of very small anions for which most of the negative charge resides on a single small (first or second row) atom as is the case for any method which does not include diffuse basis functions. Second, MNDO tends to overestimate core-core repulsions between atoms especially when they are separated by approximately their van der Waals distance. This error leads to the failure of MNDO to reproduce hydrogen bonds and to erroneous heats of formation for strained or crowded molecules.¹⁷ It is also the major cause for gross overestimates of transition-state energies and distortions of

support than his earlier work. Our calculations do not support this argument.

Our approach is to use MNDO molecular orbital calculations to model the bonding, structure and stability of variously substituted pentacoordinate silicon anions during Berry pseudorotation.¹³ We have studied nucleophilic attacks on tetramethylsilane and trimethylsilanol to form pentacoordinate adducts and the subsequent pseudorotation of the stable adducts. This has enabled us to relate the electronic nature of the various substituents to the stability and accessibility of different isomeric forms of these anions, and thus to the stereochemistry of nucleophilic substitution.

CALCULATIONS

The calculations were performed with the MNDO method developed by Dewar and coworkers.¹⁴ The MNDO method is a semi-empirical molecular orbital method based on a neglect of diatomic differential overlap (NDDO) scheme. It is parameterized by comparisons with experimental data in the form of heats of formation, molecular geometries, ionization potentials, and dipole moments for a small, "basis set" of molecules. This method, in the form of a computer program called MOPAC¹⁵, is capable of optimizing geometries of stable molecules or transition states, or modelling reaction progress along selected reaction coordinates. Options are also available to carry out force constant and thermodynamic calculations on selected geometries. MNDO is parameterized for all second row

barriers to pseudorotation in order to rationalize the observed stereochemistry. Neither choice is supported by experiment. So we began a theoretical study of pseudorotation at pentacoordinate silicon to help clarify the relationship between the stereochemistry and pseudorotation.

A currently popular theoretical interpretation of this silicon stereochemistry by Ahn and Minot involves a S_N2 transition state in which frontier orbital HOMO-LUMO interactions of an attacking nucleophile with the silicon atom and the leaving group favors either frontside attack giving retention or backside attack giving inversion.¹⁰ In this way the major dependence on the nature of the leaving group and the secondary dependence on the nature of the nucleophile are accounted for based on the sizes and hardnesses of the nucleophile and leaving group producing favorable or unfavorable HOMO-LUMO interactions. Even though the qualitative predictions of this model as applied by Corriu and Guerin¹¹ are attractive, the model ignores the fact that these stable intermediates are expected to form with minimal activation energy so there is no barrier either to attack backside or frontside. Recognizing the importance of the pentacoordinate intermediate to silicon chemistry, Minot¹² suggested that the ease of decomposition of the pentacoordinate adduct is related to the effect of the nucleophile on the adduct HOMO. His argument is that orthogonal bonds are weakened relative to opposite bonds by a hard nucleophile while the reverse happens for a soft nucleophile. This interpretation has gained much less experimental

Reasonably, an intimate relation between the stability of pentacoordinate silicon intermediates and the unique stereochemistry for nucleophilic substitution is expected. The stereochemical fate of the pentacoordinate intermediate is determined by the relative rates for dissociation, for additional nucleophilic attack and for pseudorotation. We will report mechanisms for dissociation of pentacoordinate silicon anions in a following paper. In the case of additional nucleophilic attack on the 5-coordinate adduct, if formation of a hexacoordinate silicon transition state is important as is expected for electronegative substituents then racemization is the expected stereochemical outcome for nucleophilic substitution. The hexacoordinate transition state seems a likely candidate for explaining the second-order, nucleophile-induced racemization of halosilanes.¹ In this study we have focused on formation and intramolecular isomerization by Berry pseudorotation for pentacoordinate intermediates. In cases for which a pentacoordinate intermediate is not stable, nucleophilic displacements at silicon are expected to proceed through a S_N2 type reaction with a low activation barrier for which inversion is the likely stereochemical outcome.¹ When a stable pentacoordinate intermediate is formed either inversion or retention of configuration is possible. Since nearly exclusive inversion of configuration or retention of configuration are frequently observed, one may be tempted either to discount the stability of the appropriate pentacoordinate intermediates in which case intramolecular isomerization is unimportant or to imagine large

icon chemistry is given by West and Barton.² A good starting place for understanding stereochemistry of nucleophilic substitutions at silicon is a comparison with carbon.

Reactions of nucleophiles at silicon are distinctly different from nucleophilic attack at carbon in two general ways. First, silylenium ion intermediates are rare in silicon chemistry³ compared to the important place of carbenium ion intermediates in carbon chemistry because of energetically more favorable alternatives for silicon. Second, the coordination number of silicon is readily expanded beyond four⁴ while the coordination number of carbon is not. Electronegative substituents stabilize higher coordination numbers of silicon.⁴ In fact, many nucleophiles add to tetravalent silicon in the gas phase without activation^{5,6,7} in contrast to large activation energies generally required to form pentacoordinate carbon.⁸ Stable pentacoordinate silicon anions are formed at every collision in gas phase flowing after glow experiments⁶ and they are readily observed in liquid solvents of low polarity using NMR.⁹ The reasons for these differences between silicon and carbon are the comparatively large size of the silicon atom and the possibility of d-orbital participation for silicon bonding. Dewar and Healy have argued for the predominant influence of the size difference over d-orbital participation based on MNDO molecular orbital calculations which neglect d-orbitals.⁵ Regardless of which effect dominates, all of this evidence points to the stability of pentacoordinate intermediates as a key feature of nucleophilic substitution at silicon.

CHAPTER 5

QUANTUM-CHEMICAL STUDY RELATING PSEUDOROTATION TO THE STEREOCHEMISTRY OF NUCLEOPHILIC SUBSTITUTION AT SILICON

Larry W. Burggraf and Larry P. Davis

ABSTRACT

MNDO molecular orbital calculations are used to predict stability trends for pentacoordinate anion adducts formed by nucleophilic attack on methylsilanes. Stabilities increase with increasing gas phase proton affinities of the nucleophiles. Adducts of nucleophiles with proton affinity less than chloride are not stable. Calculations of Berry pseudorotation barriers suggest that only pseudorotation about a soft pivotal ligand gives barriers substantially greater than 5 kcal/mol. A model for nucleophilic substitution at silicon is proposed for which barriers larger than the energy of the separated products are dissociative. The qualitative features for the stereochemistry of nucleophilic attack at silicon can be explained by this model.

INTRODUCTION

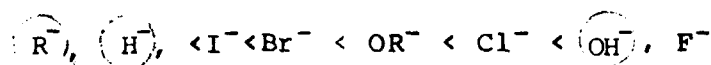
A unique aspect of silicon chemistry is the variable stereochemistry for nucleophilic substitution at silicon depending on leaving group, nucleophile and solvent. We will not review the experimental literature for silicon stereochemistry because it has been extensively reviewed and correlated by Corriu et al.¹ A good condensed summary of this stereochemistry and other features of sil-

REFERENCES

1. Fife, D.J.; Moore, W.M. *Photochemistry and Photobiology* 1979, 29, 43.
2. Oster, G.; Wotherspoon, N. *J. Am. Chem. Soc.* 1957, 82, 5602.
3. Mauzerall, D. *J. Phys. Chem.* 1962, 66, 2531.
4. King, W.F. Ph.D. Dissertation, Utah State University, Logan, UT 1973 and references therein.
5. Moore, W.M.; Baylor, C., Jr. *J. Am. Chem. Soc.* 1969, 91, 7170.
6. Moore, W.M.; Ireton, R.C. *Photochemistry and Photobiology* 1977, 25, 505.
7. Fife, D.J. M.S. Thesis, Utah State University, Logan, UT 1977.

Our calculations predict exactly such a reaction profile with a barrier of 3 kcal/mol for pseudorotation of SiF_5^- . The size of this barrier is similar to pseudorotation barriers of about 5 kcal/mol for simple ligands on TBP phosphorus. Pseudorotation of unsymmetrically substituted TBP silicon anions produce distorted reaction profiles which can be related to the size and polarizability, i.e. hardness, of ligands.

Pseudorotation profiles for $\text{Si}(\text{CH}_3)_4\text{X}^-$ vary in a regular way depending on the hardness of the ligand, X. For example, Figure 2 shows the BPR profiles for a hard ligand, F, and Figure 3 is the BPR profile for the soft ligand, H. These represent cases near the extremes of polarizability for ligands which form stable adducts. For both ligands BPR carries the X ligand from the apical to equatorial positions with a small activation barrier suggesting that BPR is labile for stable silicon adducts. In the equatorial position the H adduct is less stable and the methyl ligands crowd the H ligand distorting the geometry. The BPR for which H is in the pivotal equatorial position has a much higher activation barrier. But for the hard F ligand, the difference in the two BPR profiles is not pronounced. The trend for ligands having intermediate hardness is presented in Table 3. After we eliminate those ligands which do not form stable adducts this trend follows that given by Pearson et al.²⁰ for hardness of anions:



----->

soft

hard

Ions which are predicted to form stable adducts are circle.

The change in bond length with bond angle during the course of pseudorotation is shown for BPR of the hydroxide adduct in Figure 4. The hydroxide adduct exhibits a profile with shape intermediate between that of the fluoride and hydride adducts. The activation barrier is associated with the repulsion between CH_3 groups as the tetragonal pyramidal transition state is formed. Drastic changes in bond lengths and occur over a very small region of the reaction coordinate as the transition state snaps into the product isomeric form. Consideration of Figure 1 makes it clear that as the BPR motion snaps through the transition state that the motion is parallel to the bond between the pivotal equatorial ligand and the silicon atom exciting a normal vibrational mode in the equatorial plane in the direction. A high probability for energy transfer from the pseudorotation mode to the translational mode is expected because of the comparatively high density of states for translation. In this way energy is directed into translational motion in the equatorial plane if the equatorial bond energy is exceeded.

Pseudorotation profiles for $\text{XSi}(\text{CH}_3)_3\text{OH}^-$ anions, summarized in Table 4, are only slightly different. While the Cl^- adduct of $\text{Si}(\text{CH}_3)_4$ was unstable, its adduct with $\text{Si}(\text{CH}_3)_3\text{OH}$ was marginally

stable as shown in Table 2. The adduct eliminated Cl^- when the energy exceeded the energy of the elimination products. Presence of the harder OH ligand further destabilizes the equatorial H ligand. Notice that the softer the equatorial substituent is the more distorted is the TBP geometry.

These calculations suggest that BPR is a low energy labile process except for the situation for which a very soft ligand is in the pivotal equatorial position in which case the barrier is much larger. The picture is that of motion on a pseudorotation potential surface having large saddle-type barriers for soft ligands remaining equatorial. Motion over these higher-energy transitions are dissociative when the BPR transition state energy exceeds the stability of the adduct, producing the products of the substitution reaction as the energy is localized into translational motion of a ligand. The regions of motion on this surface are thereby limited as are the possible stereochemical outcomes.

Stereochemistry and Pseudorotation

Consider the relationship between the predicted pseudorotation profiles for stable adducts and the stereochemistry of nucleophilic substitution at silicon. We postulate a model for stereochemical control of nucleophilic substitution by the Berry pseudorotation potential surface. In this model BPR paths smaller than the dissociation energy are labile while the others are dissociative. In particular, barriers for which soft ligands are the equatorial pivot

in BPR are dissociative. The stereochemical implications of this model for a pentacoordinate silicon adduct having both a hard (h) and soft (s) ligand are presented in Figures 5 and 6. The pseudorotation nomenclature P(1,3) represents a BPR which carries equatorial ligands 1 and 3 into apical positions.

In Figure 5, possible BPR isomerizations following backside attack of substituent h or s are shown. The figure represents the entirety of the accessible BPR potential surface. Circles represent products of dissociative paths in which either a soft (s) or hard (h) leaving group is lost. In this representation, isomers (A), (B), (C), and (D) are stable points on the potential surface while those isomers represented in column 1 and column 3 are metastable or unstable points of low energy on the potential surface. The outcome of a dissociative BPR following loss of the leaving group, either retention (R) or inversion (I), is shown in the circles. In all cases for which the soft ligand is the leaving group retention of configuration is invariably the stereochemistry result. Hard ligands are invariably lost from the equatorial pre-pseudorotation position with inversion (column 2) and from the apical pre-pseudorotation position with retention in this scheme. Loss of a hard leaving group, h, may result in either inversion or retention depending on its hardness.

The effect of increasing hardness of leaving group h on the stereochemistry can be seen by considering how activation energies for BPR depend on hardness of the ligand. As the hardness of h

increases the isomers in column 2 with h equatorial are more stable. The barrier for equatorial-to-equatorial BPR for h is reduced with increasing hardness, while barriers for h going equatorial-to-apical are increased. The combined effect makes transitions from column 2 to column 1 more probable relative to transitions from column 2 to column 3 favoring inversion. Conversely, when the hardness of h is reduced, equatorial-to-axial transitions for h ligands are much more favorable and probability for transitions from column 2 to column 3 are enhanced favoring retention, which corresponds to the observation that increasing inversion accompanies increased hardness of the leaving group.¹ The observation that for the same leaving group, a nucleophile with highly localized charge is more likely to give retention than one with delocalized charge is related to the decrease in the stability of the adduct for addition of nucleophiles with smaller proton affinity. For these situations other barriers also may become dissociative and the percent inversion increases up to the extreme case for a nucleophile that does not form a stable adduct for which we predict complete inversion of configuration because only backside attack produces the proper leaving-group translational motion for dissociation. Corriu et al¹¹ point out that this trend is also consistent with the effect of solvents and complexing agents on the stereochemistry.

Figure 6 shows the corresponding situation for frontside attack of a hard or soft nucleophile. Again, total retention of configuration is predicted for a soft leaving group although BPR is labile.

In fact, this figure represents the same BPR potential surface as Figure 5 from the point of view of another starting place. All of our previous arguments also apply to pseudorotation following front-side nucleophilic attack shown in Figure 6.

This model successfully encompasses the qualitative features of the stereochemistry for simple nucleophilic attack at silicon. Although the magnitude of calculational errors do not warrant a quantitative comparison of the adduct stability with BPR barriers to predict ratios of inversion-to-retention for intermediate systems, the general features of the model invite experimental comparisons.

CONCLUSIONS

Calculated trends of stability for nucleophile adducts to tetramethylsilane and trimethylsilanol correspond to the order of nucleophile proton-affinity in good agreement with experimental trends for stability of pentacoordinate silicon anions. Calculated barriers to Berry pseudorotation are 5 kcal/mol or less except for the case in which a soft ligand occupies the pivotal equatorial position. This BPR path is the most likely one to be dissociative. We propose a model rationalizing the stereochemistry of nucleophilic attack at silicon based on these calculations. The model assumes that the pseudorotation potential surface controls the stereochemistry for stable adducts because only pseudorotation paths that produce translational energy which exceeds the energy of the separated products are dissociative. This model successfully encompasses

experimental trends of stereochemistry for nucleophilic substitution and trends of gas phase and solution phase stabilities for pentacoordinate silicon anions.

TABLE 3

PSEUDOROTATION OF X-Si(CH₃)₄⁻

	REACTION:		PSEUDO-ROTATE	
<u>X</u>	ΔH° (KCAL/MOL)		ΔH^\ddagger (KCAL/MOL)	
H ⁻	0		13.2	
OCH ₃ ⁻	0		9.2	
OH ⁻	0		7.1	
F ⁻	0		4.8	

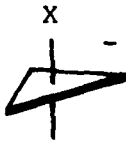
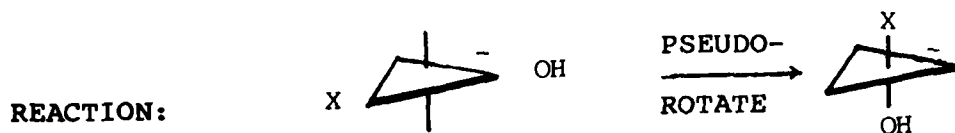
	REACTION:		PSEUDO-ROTATE	
<u>X</u>	ΔH° (KCAL/MOL)		ΔH^\ddagger (KCAL/MOL)	
H ⁻	-3.6		0.7	
OCH ₃ ⁻	-4.2		0.4	
OH ⁻	-1.9		1.7	
F ⁻	-0.4		3.1	

TABLE 4

PSEUDOROTATION OF $X-Si(CH_3)_3OH^-$



<u>X</u>	Reactant X-Si-C Angle ^{eq}	ΔH° (kcal/mol)	ΔH^{\ddagger} (kcal/mol)
H ⁻	111 ^o	-5.5	0
OCH ₃ ⁻	115 ^o	-5.2	0.1
OH ⁻	118 ^o	-3.4	1.5
F ⁻	118 ^o	-2.2	3.5
Cl ⁻	Elimination of Cl ⁻ upon pseudorotation		

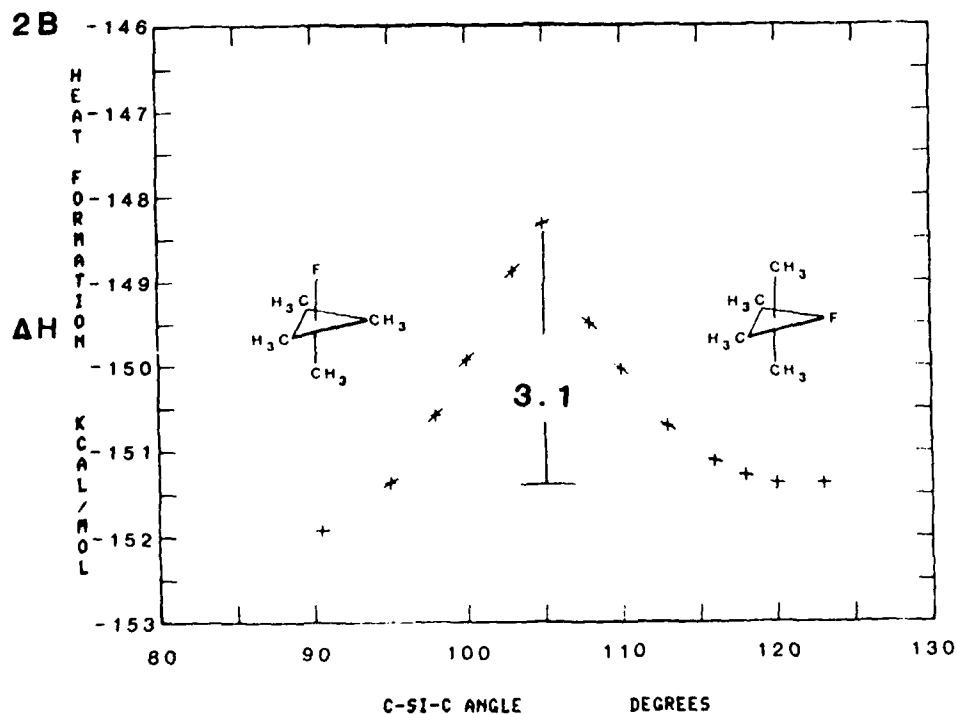
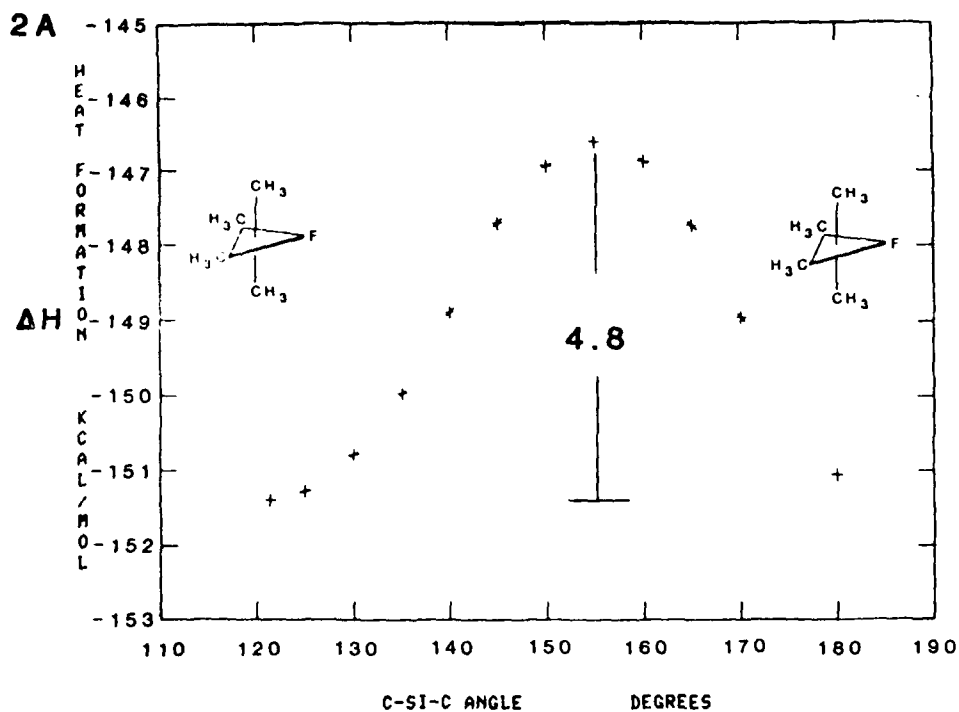


Figure 2. Berry pseudorotation profiles for fluoride adduct of tetramethylsilane. Profile 2A shows F remaining in the pivotal equatorial position. In profile 2B, F moves from an apical to an equatorial position.

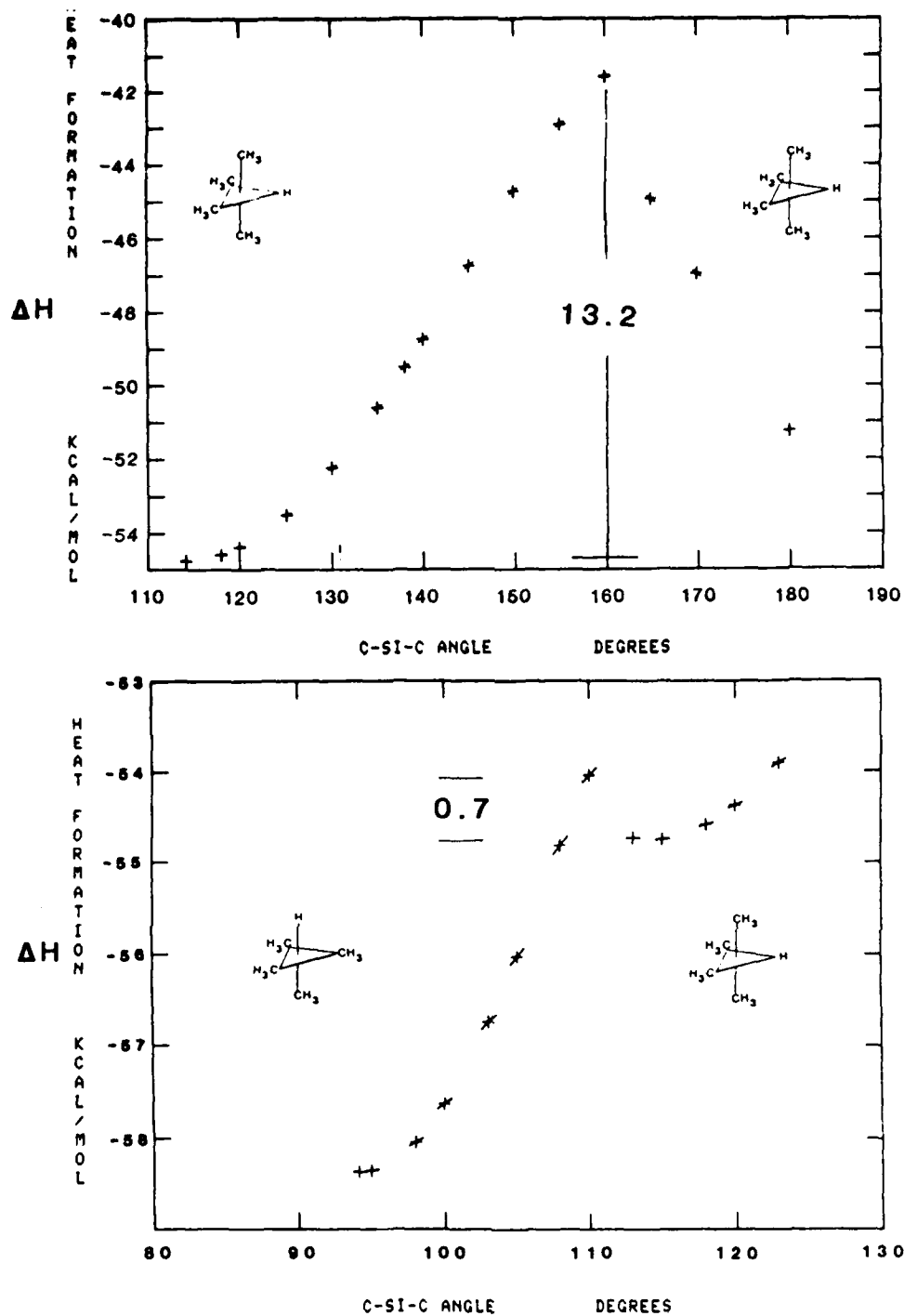


Figure 3. Berry pseudorotation profiles for hydride adduct of tetramethylsilane. Profile 3A shows H remaining in the pivotal equatorial position. In profile 3B, H moves from an apical to an equatorial position.

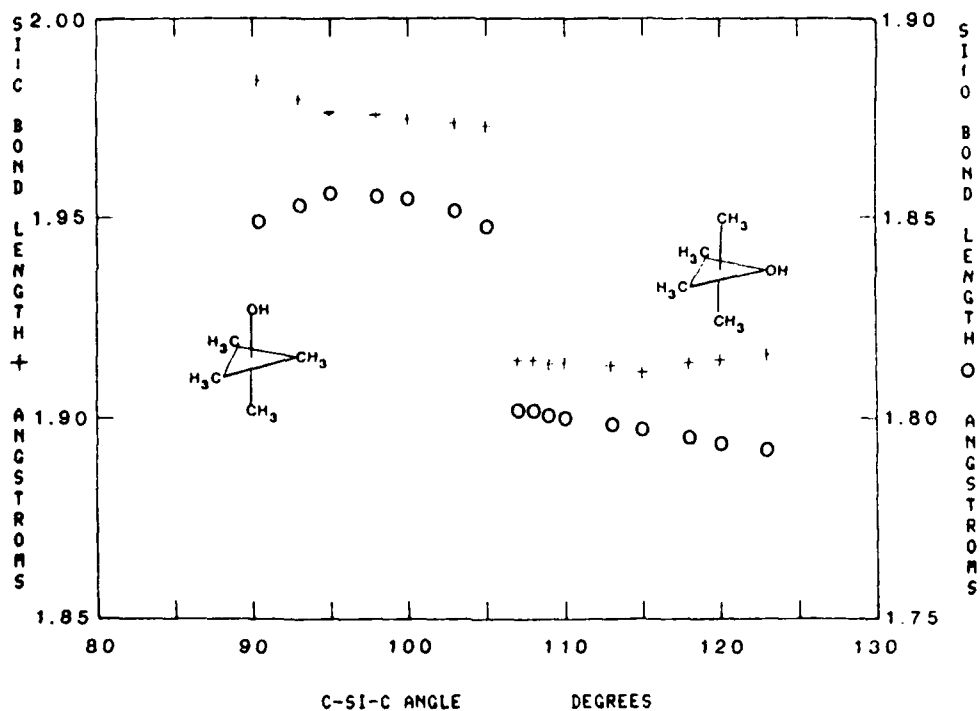
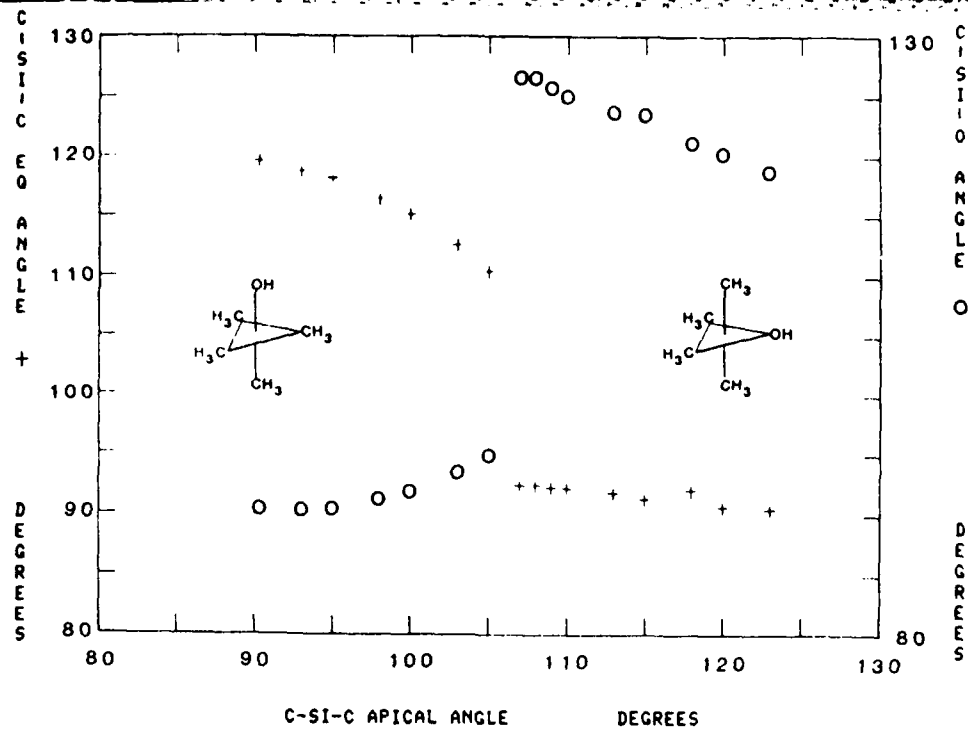
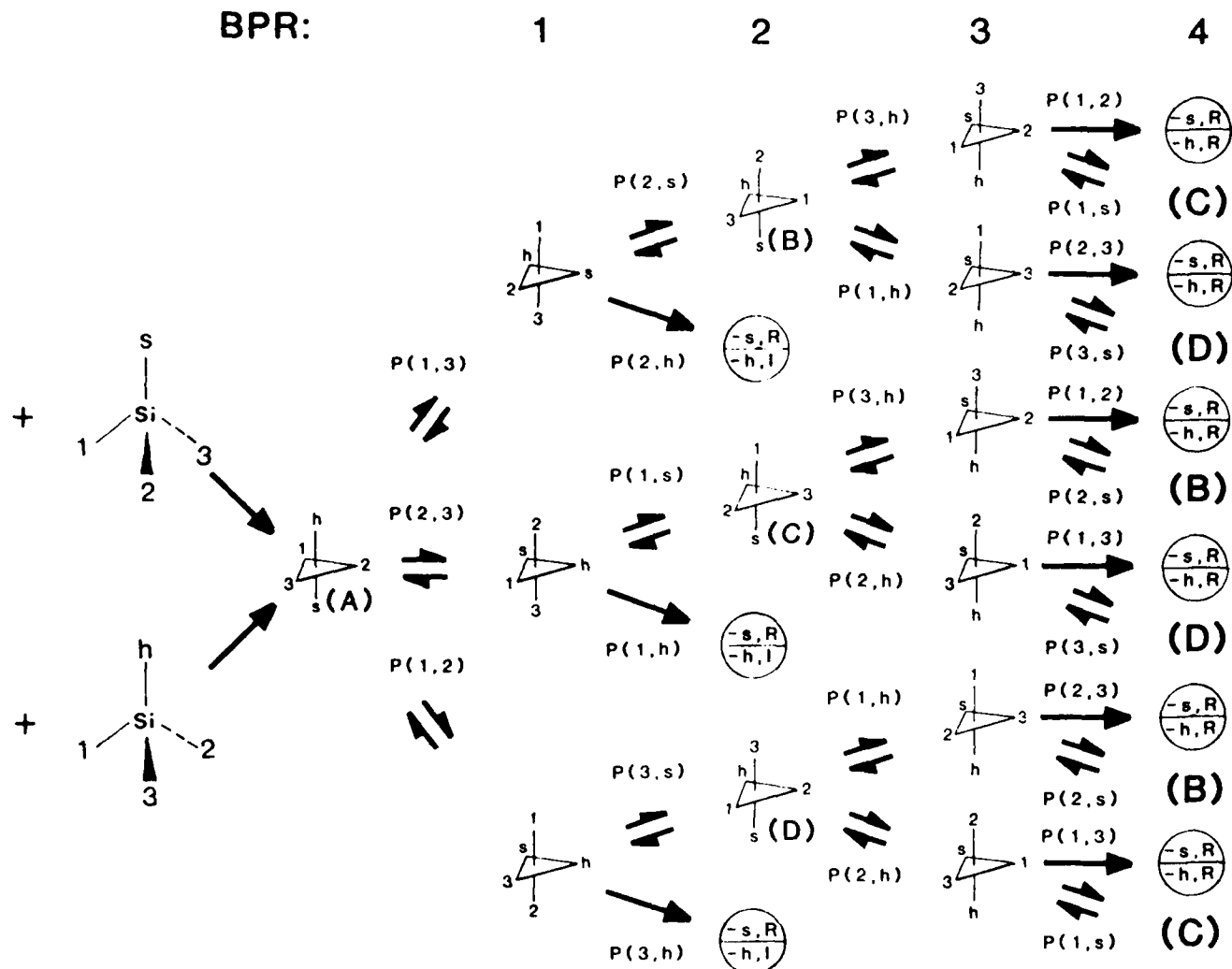


Figure 4. Bond angles as a function of reaction coordinate, the C-Si-C bond angle between apical and pivotal equatorial carbon-silicon bonds for pseudorotation of $(\text{CH}_3)_4\text{SiOH}^-$ anion. The Si-O and Si-C_e bond lengths as a function of reaction coordinate during pseudorotation. The maximum of the pseudorotation barrier is at 105° along the reaction coordinate.



PSEUDOROTATION FOLLOWING BACKSIDE ATTACK

Figure 5. Pseudorotation isomers following backside attack of hard (h) or soft (s) substituent on silane assuming that only pseudorotations for pivotal s produce dissociation with retention (R) or inversion (I) of configuration. Structures (A), (B), (C), and (D) represent stable points on the surface.

Chapter 7

Synthesis of Metallametalloenes

by Hans J. Mueh and Silvia A. Beatty

ABSTRACT

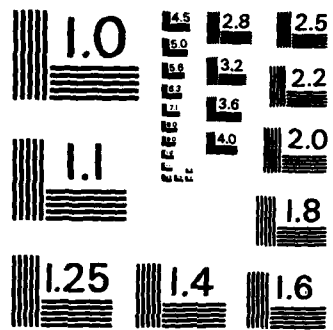
Reaction of thiophene with $\text{Fe}_3(\text{CO})_{12}$ has been shown to produce $\text{Fe}(\text{CO})_3\text{C}_4\text{H}_4\text{Fe}(\text{CO})_3$. Further treatment with $\text{C}_5\text{H}_5\text{Co}(\text{CO})_2$ yields the erracobaltocene species $\text{C}_5\text{H}_5\text{CoC}_4\text{H}_4\text{Fe}(\text{CO})_3$. This project was an attempt to synthesize and examine that compound and the isostructural species $\text{C}_5\text{H}_5\text{FeC}_4\text{H}_4\text{Fe}(\text{CO})_3$ and $\text{C}_5\text{H}_5\text{NiC}_4\text{H}_4\text{Fe}(\text{CO})_3$. The species were to be studied in an attempt to determine the effect on the carbonyl stretching frequencies and variation of the electron density around the metal center using infrared spectroscopy for the former and cyclic voltammetry for the latter. Successful syntheses have yet to be developed for the compounds.

THEORY

The metallametalloenes are a recent off-shoot of the class of synthetic compounds known as metallocenes. The first metallocene to be synthesized and characterized was the stable orange compound bis(cyclopentadienyl)iron(II) or ferrocene, shown below.

Ferrocene

Fe



MICROCOPY RESOLUTION TEST CHART
NATIONAL BUREAU OF STANDARDS-1963-A

Ferrocene was the first known compound in which a metal atom was bound aromatically to carbon rings.

A good indicator of the feasibility and stability of an organometallic compound is the Effective Atomic Number (EAN) Rule¹. This rule basically states that compounds in which the valence shell of the metal is filled are more likely to exist and to be stable. For the first row transition metals the valence shell consists of the 4s, 4p, and 3d orbitals. For the first row transition metals 18 electrons are needed to fill the valence shell, providing stability.

Ferrocene obeys the 18 electron rule as shown in the example below.

19. JANAF Thermochemical Tables, Dow Chemical Company: Midland, MI, 1965, and updates.

20. Pearson, R.G., Ed. "Hard and Soft Acids and Bases," Dowden, Hutchinson, and Ross: Stroudsburg, PA, 1973.

CHAPTER 6

THEORETICAL STUDIES OF THE PEPTIDE BOND

Larry D. Strawser, Larry P. Davis, and William Beninati

ABSTRACT

The dipeptide glycylglycine was used to model the peptide bond as a test of the MNDO method. The characteristics considered were peptide bond length, degree of planarity, barrier to rotation, and ΔH of rotation. The species considered were the neutral form, the +1, -1, and zwitterionic form. Our results showed that MNDO does provide a realistic model of the peptide bond.

INTRODUCTION

The Air Force has an interest in understanding a class of weapons that work against the neuromuscular junction of a human, disabling and then killing him. These agents block the active site of the enzyme acetylcholinesterase which enables the transmission of nerve impulses across the junction by hydrolyzing acetylcholine. It is felt that a better understanding of the active site interaction could lead to a possible antidote. Therefore, we are undertaking a long term effort to model the active site of acetylcholinesterase. We are using the MNDO semi-empirical method¹, rather than an ab initio method because of the complexity of the system. Since no

theoretical method has been tested on a system of this complexity, we do not know if MNDO will accurately model the salient structural or mechanistic features of the active site interaction.

Our approach to this problem begins with an assumption that most enzyme-substrate interactions follow the same basic mechanism -- the solvactivated mechanism proposed by Dewar^{2,3}. We will test our methodology by modeling another enzyme interaction, which presumably follows the same solvactivated mechanism, and on which more data is available. The enzyme we chose is alpha-chymotrypsin.

Alpha-chymotrypsin is a digestive enzyme whose normal function is to cleave the peptide bonds of proteins. Proteins are hydrolyzed by this enzyme only at those peptide bonds in which the carboxyl group is contributed by a phenylalanine, tryptophan, or tyrosine residue. The enzyme will also hydrolyze the ester linkages of a number of artificial substrates, including p-nitrophenyl acetate, whose products of hydrolysis can easily be assayed colorimetrically. A large body of structural and kinetic data is available for the enzyme^{4,5,6}. This is data we will use for comparison with the MNDO model. The model cannot be complete, however, unless it includes a good model of the peptide bond -- the most reactive substrate group. This study is a test of the MNDO model of the peptide bond. We chose the simplest example of a peptide -- glycylglycine, and modeled the neutral, +1, -1, and zwitterion species.

THEORETICAL CALCULATION METHODS

The object of theoretical calculation methods is to find the set of solutions to the Schroedinger equation for the molecule being considered. It is not possible to do this analytically, but an approximation can be reached using the linear combination of atomic orbitals, and a self-consistent field calculation. Beyond this basic scheme, MNDO employs a valence basis set, with neglect of the electron repulsion integrals involving diatomic differential overlap. MNDO is also a semi-empirical method¹. The program is parameterized with experimentally determined heats of formation and geometries¹. The parameterization greatly improves the accuracy of the method, but limits calculations to the elements which have been parameterized.

Calculations are run for a given molecule starting with an initial geometry estimated by the user. This geometry is defined in terms of a set of internal coordinates and then input to the program. MNDO provides a number of different outputs to the user, including optimized geometries, bond orders, localized orbitals, and heats of formation⁷.

We began our peptide bond study by optimizing the cis and trans isomers of each form of glycyglycine that we considered. Then we calculated heats of formation at points along the reaction coordinate for rotation around the peptide bond, between the trans and cis dipeptides. From plots of these reaction coordinates we could estimate the transition state geometry (particularly the

dihedral around the peptide bond). Then MNDO located the transition state using a non-linear least squares gradient minimization routine⁷. This routine will locate three types of stationary points: 1) minima in the energy surface, 2) transition states, and 3) any other stationary points in the gradient norm space⁷. By our initial guess we improve the chance that the point we find will be the transition state, but we can test our results by doing a force constant calculation on the stationary point. One negative force constant with all other force constants positive will indicate that we have calculated the geometry and heat of formation for a saddle point⁷.

These calculations will give us calculated values for the data that we are considering in this study: peptide bond length, bond order, degree of planarity, delta H for trans to cis rotation, and the barrier to such rotation.

RESULTS AND DISCUSSION

Table 1 presents the results of the MNDO calculations for the most stable form of glycylglycine in its different charged configurations, which are shown in Figure 1. In solution, at physiological pH's, we would expect a zwitterionic form to be present, with the carboxyl group negatively charged, and the amino group positively charged. Unfortunately, since MNDO (as do all molecular orbital methods) only calculates the properties of

TABLE 1

MNDO Geometries of the Peptide Bond in Glycylglycine

<u>Quantity</u>	<u>Experimental</u>	<u>Neutral</u>	<u>+1 ion</u>	<u>-1 ion</u>
Bond Length (angstroms)	1.33 ⁸	1.41	1.39	1.41
Twist Angle (degrees)	5-6 ⁹	6	10	35

TABLE 2

Energetics of Peptide Bond Rotations

<u>Quantity</u>	<u>Experimental</u>	<u>Neutral</u>	<u>+1 ion</u>	<u>-1 ion</u>
ΔH (kcal mol ⁻¹)	>0	2.0	1.6	0.4
E_a (kcal mol ⁻¹)	>0	8.5	9.9	7.4

Figure 1. Different charge configurations of glycylglycine.

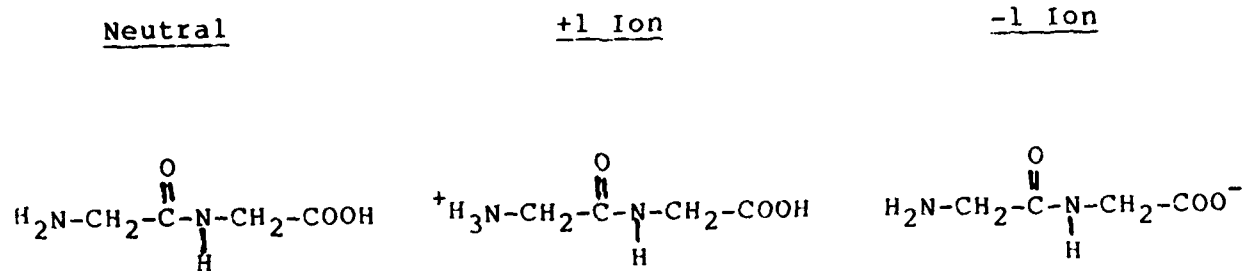


Figure 2. MNDO-calculated structure for the neutral form of glycylglycine.

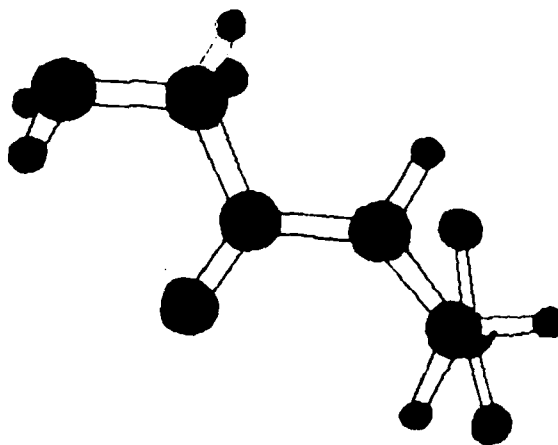


Figure 3. Optimized geometries of glycylglycine of points on the peptide bond rotation reaction coordinate.

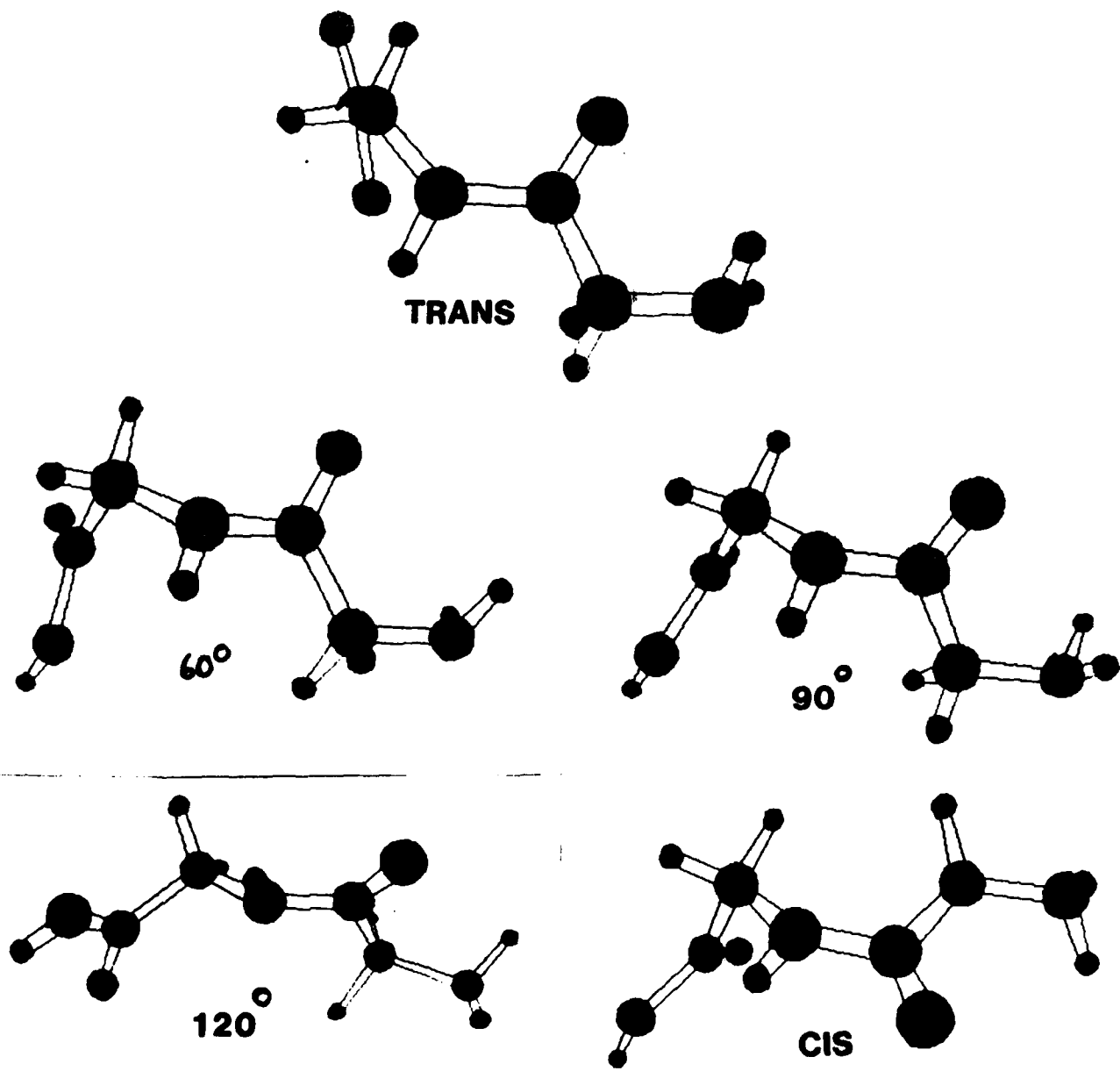
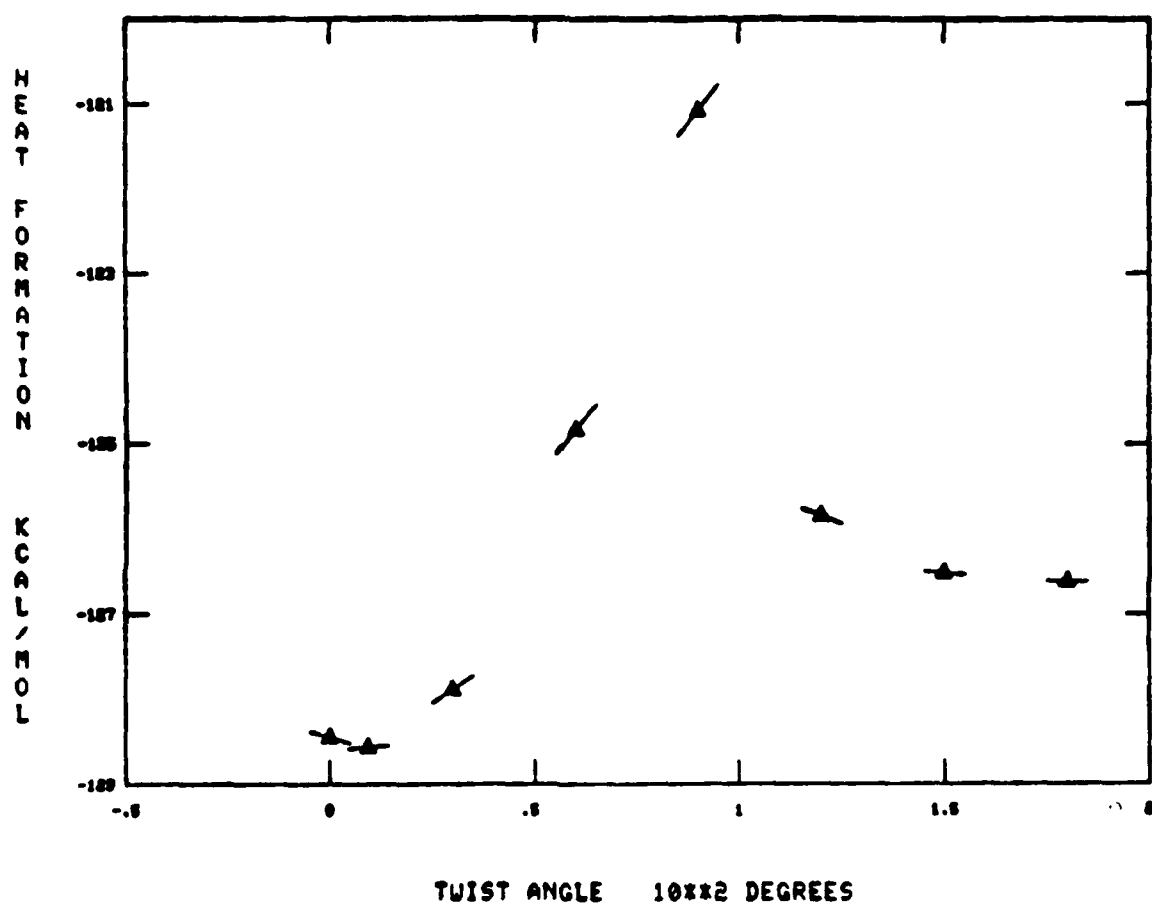


Figure 4. Energy profile of peptide bond rotation of neutral glycylglycine.



isolated molecules (analogous to the gas phase), attempts to form the zwitterion invariably lead to abstraction of a proton from the positively charged NH_3^+ amino group by the negatively charged COO^- carboxyl group. Even attempts to neutralize the two charges with simulated counterions could not prevent this from occurring.

The table shows that the peptide bond length predicted by MNDO is longer than the experimental value by several hundredths of an angstrom. Still, the agreement is fairly good, considering that the experimental data is for long polypeptide chains in a crystalline environment. MNDO also correctly predicts the near-planarity of the group attached to the peptide bond linkage. The complete MNDO structure for the neutral form of glycylglycine is shown in Figure 2.

In order to study the barrier to rotation around the peptide bond, we calculated optimized geometries for a series of partially rotated structures, shown in Figure 3 for the neutral form. Figure 4 shows the energy profile obtained from this reaction path calculation. In each case, the highest energy point is revealed at a rotation angle of slightly greater than 90 degrees, as we would expect from breaking a partial pi-bond. The calculated activation energies and the differences in energies between the cis and trans forms are given in Table 2. The barrier to rotation appears to be on the order of 7 to 10 kcal mol⁻¹, with the trans form (with the C=O and the N-H groups trans to each other) predicted correctly to be slightly more stable than the cis form.

CONCLUSIONS

MNDO appears to do quite well in calculating the essential features of the peptide bond, including both geometries and energetics. We are continuing work to include a more realistic model, including solvent effects, crystals effects, and a polymeric model of the polypeptide chain. We feel confident that polypeptides and their reactions can be modelled successfully with MNDO and its successors.

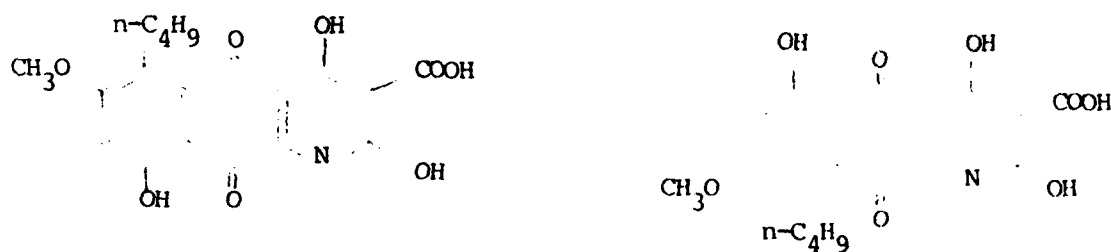
REFERENCES

1. Dewar, M.J.S. and Walter Thiel, "The MNDO Method. Approximations and Parameters", J. Am. Chem. Soc., 99, 4899-4907 (1980).
2. Dewar, M.J.S., "A New Approach to Enzyme Reactions", Proc. Nat. Acad. Sci., in press.
3. Dewar, M.J.S., "Solvent Effects in Substitution Reactions; A Reinterpretation of HSAB Theory", Unpublished Manuscript.
4. Blow, D.M. and Steitz, T.A., "X-Ray Diffraction Studies of Enzymes", Ann. Rev. Biochem., 39, 63-100 (1970).
5. Matthews, B.W., Sigler, P.B., Henderson, R., Blow, D.M., "Three-dimensional Structure of Tosyl-alpha-chymotrypsin", Nature, 214, 652-656 (1967)
6. Oppenheimer, H.L., Labouesse, B., Hess, G.P., J. Biol. Chem., "Implication of an Ionizing Group in the Control of Conformation and Activity of Chymotrypsin", 241, 2720-2730 (1966).
7. Quantum Chemistry Program Exchange Numbers 455 and 464, Department of Chemistry, Indiana University, Bloomington, Indiana 47405
8. G.N. Ramachandran, et. al., Biochem. Biophys. Acta., 359, 298-302 (1974).
9. L. Pauling and R.B. Corey, Proc. Roy. Soc., "Stable Conformations of Polypeptide Chains", B141, 21-35 (1953A).

To the chemist this pink discoloration of the roots of the diseased plant has attracted interest. Attempts have been made to determine what compound and/or compounds are responsible for this red to pink coloration. In addition pathologists would like to know if these pigments or other metabolic by-products play a role in disease expression. Also a complete study of the biosynthesis of these pigments as well as their biological significance would add greatly to the basic knowledge of science.

PREVIOUS WORK

Kreutzer (8,9) was the first worker to study the pigment of *P. terrestris*. A few years later, Kogl and Sparenburg (10) obtained a pigment, phomazarin, $C_{19}H_{17}O_8N$ from the mycelium of this fungus. The pigment was a derivative of the heterocyclic ring system azanthracene and was allocated an azanthraquinone structure with the substituents (n-butyl), $(-OH)_3$, $(-OCH_3)$, and $(-COOH)$. Further work by Kogl, et. al. (11,12) led to the suggestion of two alternative structures (I or II).

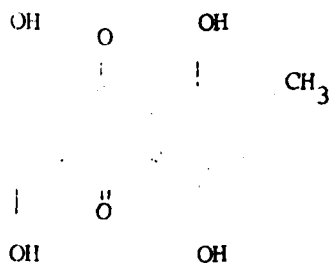


(I)

(II)

In 1960, Wright and Schofield (13) re-examined a culture of *P. terrestris* obtained from the Central Bureau voor Schimmelcultures (Baarn) and grown exactly as described in Kogl. There was isolated from the mycelium by simple extraction processes an anthraquinone compound called cynodontin (III). They were unable to isolate any

compound resembling phomazarin, although they mentioned the presence of at least one other pigment.

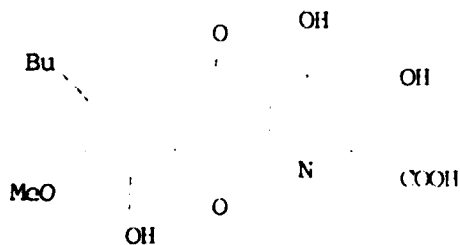


Cynodontin (III)

Birch, et. al. (14), however, found that cultures from the same source produced the pigment, phomazarin, which agree in physical properties with those described by Kogl. For reasons which they were unable to determine, the same organism grown under the usual conditions does not invariably produce this pigment. Like Wright and Schofield they observed cynodontin.

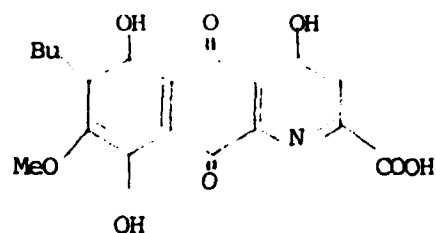
Preliminary work on the biosynthesis of phomazarin by Birch, et. al. (14) indicated that eight acetate units are involved together with a grouping arising possibly from glycine or another amino acid. The distribution of activity and spectral evidence supported structure (I) rather than (II).

Birch, et. al. (15) finally in 1979 completed structure investigations on phomazarin and have shown it to be (IV).



Phomazarin (IV)

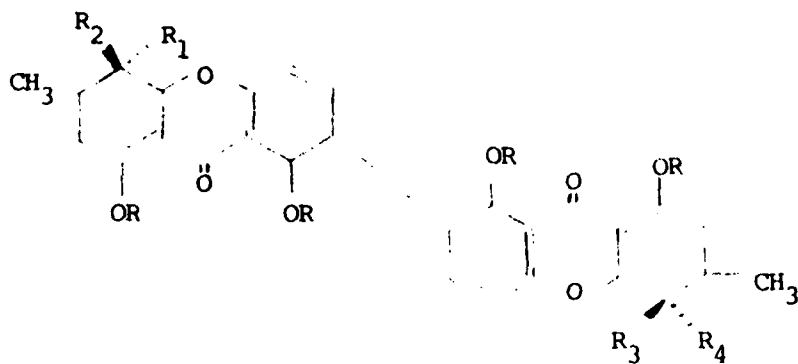
Effenberger and Simpson (16) reported the same year isolation of a small amount of pigment they termed isophomazarin (V).



Isophomazarin (V)

Five additional metabolites have also been isolated and identified from the mycelium of Pyrenochaeta terrestris (17,18).

These compounds have been called secalonic acids A, E, G, emodin, and endocrocin. Their structures are given below (VI - X).

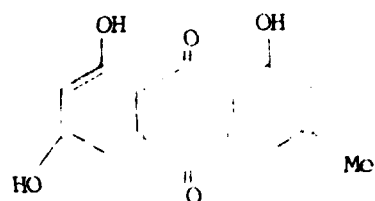


Secalonic Acid A - - - R = R₂ = R₃ = -H; R₁ = R₄ = -OH

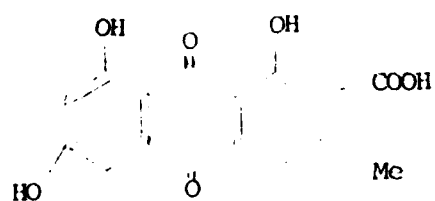
Secalonic Acid E - - - R = R₁ = R₄ = -H; R₂ = R₃ = -OH

Secalonic Acid G - - - R = R₁ = R₃ = -H; R₂ = R₄ = -OH

(VI - VIII)



Emodin (IX)



Endocrin (X)

A summary of the pigments and properties is given in Table I.

Table I. Pigments isolated from Pyrenochaeta terrestris.

<u>Pigments</u>	<u>Colors</u>	<u>MP (°C)</u>	<u>Reference</u>
Cyodontin	red	260	13
Phomazarin	orange	196	15
Isophomazarin	deep red needles	215- 216	16
Secalonic acid A	orange needles	208- 209	17
Secalonic acid E	yellow	206- 208	17
Secalonic acid G	yellow	206- 207	17
Emodin	orange plates	257- 259	18
Endocrin	reddish- orange	289- 314	18

OBJECTIVES

(1) To isolate and identify completely all the pigment materials associated with this fungus (examine the large amount of purple gum).

(2) To determine reasons why P. terrestris produces the pigment phomazarin in some instances and cynodontin at other times.

(3) To see if using different media would have any effect on pigment production.

PROCEDURES

The procedures are divided into two sections. The first section will deal with the procedures followed to grow mycelium while the second section will deal with the procedures used to isolate the pigments.

Growth of the fungus. - An isolate of Pyrenochaeta terrestris (designated as P.t.) was obtained from the American Type Culture Collection, Bethesda, Maryland. Stock cultures were carried on potato dextrose agar and transferred at regular intervals. Thirty

grams of sucrose was added to the following basal medium for growth of the fungus. The basal medium was of the following composition: $\text{MgSO}_4 \cdot 7\text{H}_2\text{O}$ - 0.5 g; KH_2PO_4 - 1.5 g; NaNO_3 - 1.0 g; 0.5 ml of a $\text{Fe}(\text{NO}_3)_3$ solution; 0.5 ml of a minor elements solution; and distilled water added to make a final volume of 1 liter. The ferric nitrate solution and minor elements solution were of such concentration that the final concentrations in a liter of medium were as follows: Fe - 0.2 mg; Cu and Zn - 0.1 mg; and Mo and Mn - 0.02 mg. Mn, Cu, and Zn were added as the sulfates and Mo as sodium molybdate. The medium was adjusted to pH 4.5 using 10 per cent sodium hydroxide and dispensed 25 ml/125 ml Erlenmeyer flask. The flasks were plugged with cotton and autoclaved 15 minutes at 1.05 kg/cm² pressure. The chemicals used were chemically pure quality obtained from commercial sources. Inoculum was prepared by transferring small mycelial biscuits from a culture growing on potato dextrose agar into several flasks of medium. The flasks were shaken gently and set aside for growth at room temperature. After 6-8 days, mycelial growth was visible. The content of these flasks were ground for 1 minute with a Waring blender and 1 ml of the suspension was pipetted into each of the test flasks. All procedures were carried out aseptically. The flasks were incubated at room temperature (25-28°C). After 21 days, the mycelial mats were harvested by filtration using cheese cloth, washed with distilled water, and then dried in 110°C oven for 24 hours. The mycelium from the starch solution was grown the same way except instead of sucrose and basal medium, a starch solution was used. The solution was composed of 50 g starch, 1 g potassium dihydrogen phosphate, 0.5 g calcium chloride and 0.001 g of ferrous sulfate heptahydrate in 1 liter of distilled water.

Extraction of mycelium. - Known quantities of dried mycelium were finely powdered using a mortar and pestle and then exhaustively extracted using a Soxhlet apparatus. The mycelium was extracted first with diethylether, acetone and then methanol. The residual mycelium was washed using 20 ml of petroleum ether. It was then air dried and acidified with 35 ml of 2 M aqueous HCl. The mycelium was repeatedly washed with water until neutral. Then the mycelium was further extracted with diethylether, chloroform and acetone. Solids from the above extracts were obtained by blowing a small stream of air over the flasks containing the solvents or by using a vacuum rotary film evaporator at a temperature no greater than 40°C. Attempts were made to recrystallize the solids from the first set of extractions (ether, acetone, and methanol) using pyridine. On the solids from the second extraction with chloroform, a mass spectra was performed using the mass spectra instrument of the Frank J. Seiler Research Laboratory. Analysis was performed by Mr. Lloyd Pflug. The solids from the chloroform extraction were next separated using preparatory silica gel thin layer chromatography.

Elution was performed with hexane, ethylacetate - (50/50, v/v) and ethylacetate - hexane (30/70, v/v). The eluant ratio of 50/50, v/v of ethylacetate - hexane gave the best results. After air drying, the different pigments were identified visually and by using a short and long wave length UV mineral light. The different pigment areas were cut from the silica gel and extracted with ethylacetate. The pigments were further isolated by filtration and evaporated of the solvent using a vacuum rotary film evaporator.

RESULTS AND OBSERVATIONS: The following results and observations are noted and given in the tables below.

Table II. First extraction of the dried mycelium of Pyrenochaeta terrestris.

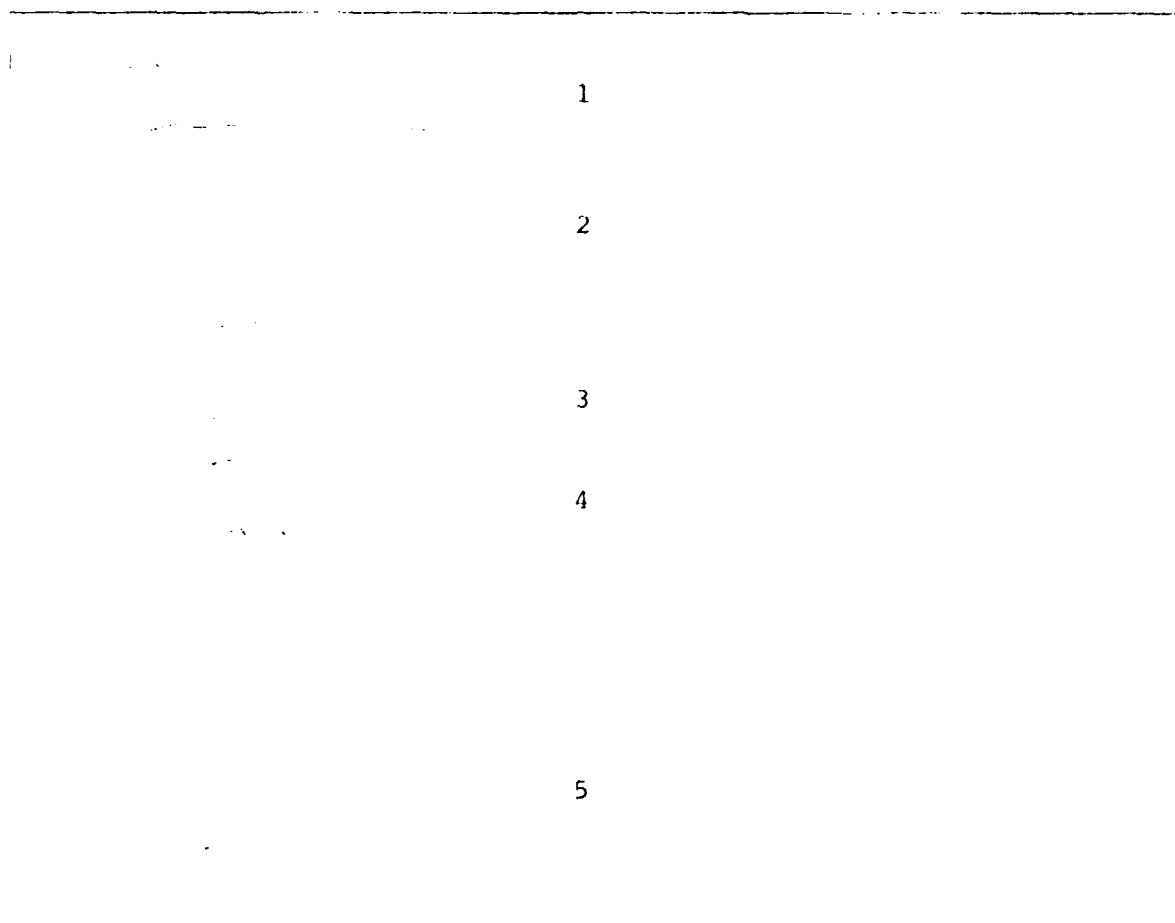
<u>Solvents</u>	<u>Solutions</u>	<u>Crystals</u>	<u>Recrystallizing solvents</u>	<u>Solids</u>
Ether	dark pink	red	pyridine	red/ purple
Acetone	red/orange	red	pyridine	red/ purple
Methanol	dark red	red	pyridine	red purple

Table III. Second extraction of the dried mycelium of Pyrenochaeta terrestris.

<u>Solvents</u>	<u>Solutions</u>	<u>Crystals</u>	<u>Recrystallization solvents</u>	<u>Solids</u>
Ether	dark orange	red/orange	pyridine	red/ orange
Chloroform	orange-yellow	red/orange	chloroform	red/ orange
Acetone	deep red	red/orange	-	-

Table IV. Diagram and comments about the thin layer chromatography of the chloroform extract of *Pyrenochaeta terrestris*. Ethylacetate - hexane (50/50,v/v) was used to develop the TLC plates.

TLC Plate

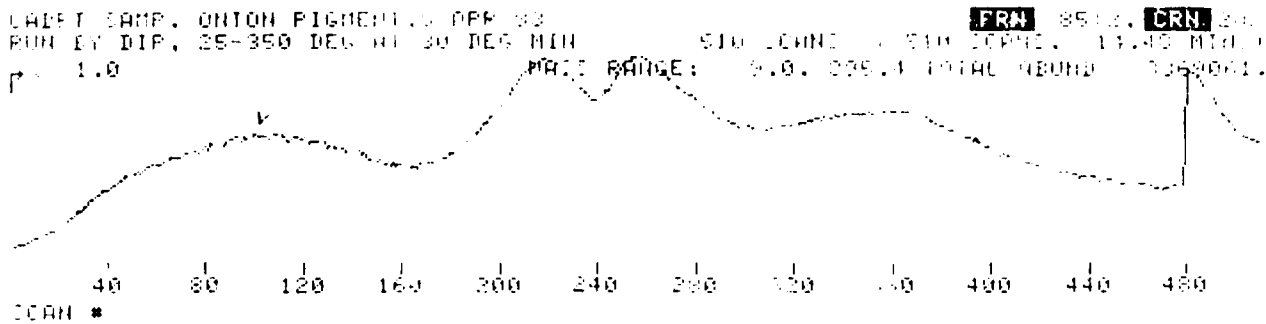


<u>Wavelengths used</u>	<u>Ethyl Acetate Solution</u>	<u>Compound</u>	<u>Silica Gel</u>	<u>No.</u>
short	yellow	oily yellow	white	1
short, long	dark pink	pink solid	white	2

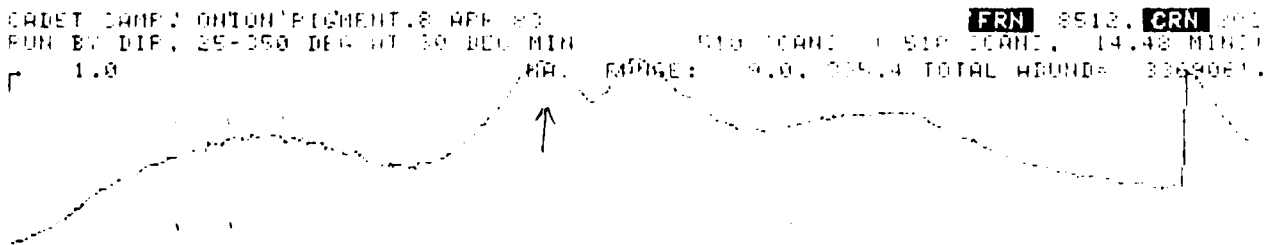
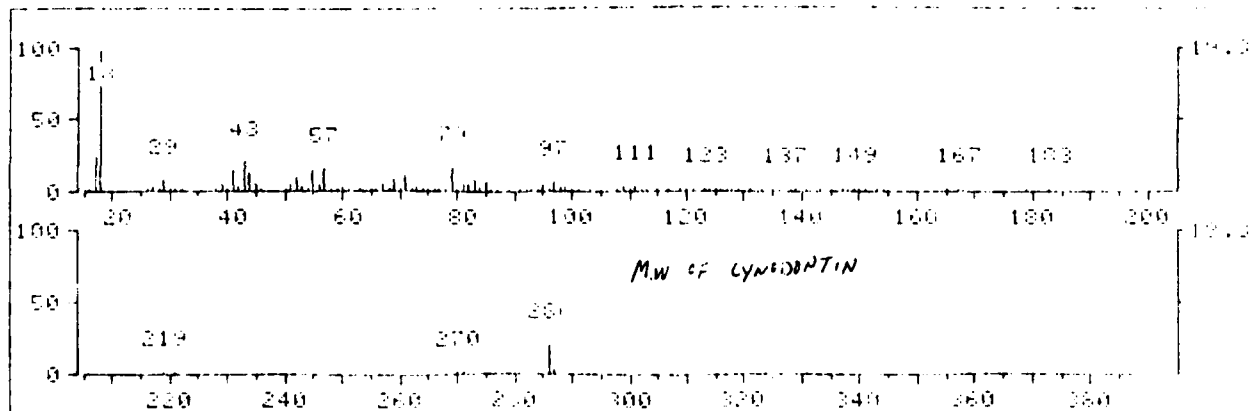
long	pink	pink solid	white	3
long	yellow	yellow solid	white	4
long	purple-red	oily yellow	pink	5

The oily compounds might indicate a mixture of different pigments. As for silica gel #5, the pink color indicated an unisolated pigment, where as white colors indicated that the pigments were separated from the silica gel. Due to lack of time attempts to further isolate the pink pigment from the silica gel strip #5 could not be performed.

Table V. Mass Spectrum of Chloroform Extract:



AVERAGED SPECTRUM * BASE PE ABUND: 18.17 32000. + 104 -1



The mass spectrum done on the chloroform extract indicated a molecular weight of 286 which is the molecular weight of cynodontin. The sole purpose of doing a mass spectrum at that time was to see if cynodontin might be present in the chloroform extract.

Growth of Mycelium

The colors of the mycelial mats were definitely different between the mycelium grown in sucrose solution and the mycelium grown in starch solution. The dried mycelium of starch source was very pink whereas the dried mycelium of sucrose source was brownish/green. According to the literature the mycelium with the higher proportion of cynodontin would have a pink color while the mycelium with a large amount of secalonic acids and cynodontin would have a brownish green color (18).

CONCLUSIONS. From the above observations it appears that at least five compounds can be isolated. Attempts to identify these compounds have not been successful. It appears visually that the starch solution favors the production of red pigments whereas the sucrose solution is favorable to the formation of other compounds. More additional work is needed to isolate and completely identify the pigments from the fungus, Pyrenochaeta terrestris.

RECOMMENDATIONS. The following recommendations are made by ClC Henry H. Shin who performed the cited work as his independent research study for chemistry 499.

1. Take pictures of research to document the work performed. These could be used as part of a presentation for the American Chemical Society Meeting in Miniature.
2. Start work in the laboratory much earlier. Two semesters of Independent Study would have given some positive results.
3. Try to identify the pigment already isolated using the tools of the organic chemist.
4. Use thin layer chromatography to separate and isolate the pigments.
5. Quantify the amounts of the pigments present in the mycelium grown using different cultural media.

REFERENCES CITED:

1. J.J. Taubehaus and A.D. Johnson, Phytopathology, 7, 59 (1917).
2. H.N. Hansen, Science, 64, 525 (1926).
3. H.N. Hansen, Phytopathology, 19, 691 (1929).
4. H.N. Hansen, Phytopathology, 19, 1135 (1929).
5. A.M. Gorenz, A.C. Walker, and R.H. Larson, Phytopathology, 38, 381 (1948).
6. W.A. Kreutzer, Phytopathology, 31, 907 (1941).
7. B.E. Struckmeyer, C.G. Nichols, R.H. Larson, and W.H. Gabelman, Phytopathology, 52, 1163 (1962).
8. W.A. Kreutzer, Phytopathology, 29, 629 (1939).
9. W.A. Kreutzer, J. Colorado Wyoming Acad. Sci., 89, 3680 (1940).
10. F. Kogl and J. Sparenburg, Rec. trav. chim., 59, 1180 (1940).
11. F. Kogl and F.S. Quackenbush, Rec. trav. chim., 63, 251 (1944).
12. F. Kogl and G.C. van Wessem, and O.I. Elsbach, Rec. trav. chim., 64, 23 (1947).
13. D.E. Wright and K. Schofield, Nature, 188, 233 (1960).
14. A.J. Birch, R.I. Fryer, P.J. Thompson, and H. Smith, Nature, 190, 441 (1961).
15. A.J. Birch, D.N. Butler, R. Effenberger, R.W. Richard and T.J. Simpson, J. Chem. Soc. Perkin Trans I, 3, 807 (1979).
16. R. Effenberger and T.J. Simpson, J. Chem. Soc. Perkin Trans I, 3, 823 (1979).
17. C.C. Howard and R.A.W. Johnstone, J. Chem. Soc. Perkin Trans I, 20, 2440 (1973).
18. I. Kurobane, L.C. Vining and A.G. McInnes, J. Antibiot (Tokyo), 32, 1256 (1979).

END

FILMED

10-85

DTIC